Distance statistics in quadrangulations with a boundary, or with a self-avoiding loop

2009 J. Phys. A: Math. Theor. 42 465208

(http://iopscience.iop.org/1751-8121/42/46/465208)

IOP PUBLISHING JOURNAL OF PHYSICS A: MATHEMATICAL AND THEORETICAL

J. Phys. A: Math. Theor. **42** (2009) 465208 (44pp) doi:10.1088/1751-8113/42/46/465208

Distance statistics in quadrangulations with a boundary, or with a self-avoiding loop

J Bouttier and E Guitter

Institut de Physique Théorique, CEA, IPhT, F-91191 Gif-sur-Yvette, CNRS, URA 2306, France

E-mail: jeremie.bouttier@cea.fr and emmanuel.guitter@cea.fr

Received 29 June 2009, in final form 21 September 2009
Published 26 October 2009
Online at stacks.iop.org/JPhysA/42/465208

Abstract

We consider quadrangulations with a boundary and derive explicit expressions for the generating functions of these maps with either a marked vertex at a prescribed distance from the boundary, or two boundary vertices at a prescribed mutual distance in the map. For large maps, this yields explicit formulae for the bulk–boundary and boundary–boundary correlators in the various encountered scaling regimes: a small boundary, a dense boundary and a critical boundary regime. The critical boundary regime is characterized by a one-parameter family of scaling functions interpolating between the Brownian map and the Brownian continuum random tree. We discuss the cases of both generic and self-avoiding boundaries, which are shown to share the same universal scaling limit. We finally address the question of the bulk–loop distance statistics in the context of planar quadrangulations equipped with a self-avoiding loop. Here again, a new family of scaling functions describing critical loops is discovered.

PACS numbers: 02.10.Ox, 05.40.−a

(Some figures in this article are in colour only in the electronic version)

1. Introduction

Understanding the properties of random maps is a fundamental question for both the mathematical and the physical community. In mathematics, maps raise at a discrete level beautiful and rather involved combinatorial problems while, at a continuous level, they give rise to new probabilistic objects, such as the Brownian map, whose construction is still under investigation. In physics, maps are used as discretizations for fluctuating surfaces in various domains ranging from low-energy physics, for instance in the context of fluid membrane statistics, to high-energy physics in the fields of string theory or of two-dimensional quantum gravity [1].

The first incursion into these problems dealt mainly with global properties of random maps. At the combinatorial level, this amounted to a precise enumeration of various families of maps by several methods developed by mathematicians or physicists. These include in particular the original approach through recursive decomposition, developed by Tutte in a series of papers [2], and the approach through random matrix integrals, which provide a systematic and powerful machinery for enumeration [3, 4]. With this latter technique, the study was extended to maps with possible extra statistical degrees of freedom such as spins or particles (see [4] for a review). At a continuous level, many results such as exponents characterizing global properties of the maps were obtained heuristically via the so-called Liouville model [5]. Beside global properties, one then addressed the more refined question of the actual dependence of correlations on the *distance* along the map. A first expression was obtained in [6] and [7] (see also [8]) for the so-called *two-point function*, which gives the law for the distance between two points on the map and more generally for the 'loop–loop propagator', measuring the distance between two boundary loops at the extremities of a cylindrical map. These results were obtained in the context of triangulations via Tutte's recursive decomposition approach, but at the price of heuristic arguments which, although non-rigorous at the discrete level, led eventually to the correct continuous correlators. Apart from this result, little remained known for quite a while on the statistics of distances in maps or, equivalently, on the metric structure of the Brownian map, probably because neither the recursive decomposition nor the matrix integral approach, nor even the Liouville model, is well suited to address questions on the distance.

Fortunately, a completely new enumeration technique was then discovered, where the distance plays a central role. It uses bijections to code the maps by much simpler objects such as the so-called *well-labeled* trees, where the labels precisely retain some of the distances in the map. This bijective approach was initiated by Schaeffer for quadrangulations (maps with tetravalent faces only) [9] and later extended to maps with arbitrary prescribed face valences [10], Eulerian maps and maps with particles or spins [11]. As far as distance statistics is concerned, a first application dealt again with the two-point function, giving the law for the distance between two vertices on the map. This law was derived exactly at the discrete level in [12] in the case of quadrangulations of fixed area and was shown to converge to a continuous universal scaling function, giving a rigorous proof of the expression of [6] and [7]. A related quantity, the radius, was discussed in [13, 14]. The universal continuous two-point function is an intrinsic characteristic of the Brownian map, a more fundamental object toward which many families of random planar maps (falling in the universality class of the so-called 2D pure gravity, such as maps with arbitrary bounded face degrees or maps coupled to non-critical statistical models) are expected to converge in the scaling limit where the area of the maps is large and scales as the fourth power of the distance [15, 16]. Transposing the Schaeffer bijection or its extensions at the continuous level allowed us to construct this Brownian map as a random metric space, which was shown in particular to be homeomorphic to the two-dimensional sphere [17, 18]. Other properties of the Brownian map could be derived by first understanding their discrete counterparts and then taking a continuous scaling limit. For instance, the statistics of geodesics (i.e. paths of shortest length) between two points was considered in [19], and it was shown that for typical points all geodesics coalesce into a unique macroscopic geodesic path in the scaling limit [20, 21]. The so-called *three-point function*, which measures the joint probability distribution for the pairwise distances between three uniformly chosen random vertices, was computed exactly in [22] in the case of quadrangulations of fixed area, and its universal scaling limit was analyzed. A remarkable property of confluence was discovered by Le Gall [21], stating that the three geodesic paths joining three typical points on the Brownian map merge by pairs before reaching their endpoints. Again, a complete characterization of

the geometry of a geodesic triangle could be obtained from an exact solution at the discrete level [23].

So far, all the above rigorous results on the distance statistics obtained via the bijective approach dealt with closed planar maps, i.e. with the topology of the sphere. In this paper, we extend these results to the more general context of maps *with a boundary*. More precisely, we are interested in the *bulk–boundary correlator*, which gives the law for the distance to the boundary of a vertex drawn at random in the bulk of the map, and in the *boundary–boundary correlator*, measuring the distance between two vertices on the boundary. Note that, in some sense, the bulk–boundary correlator lies half-way between the two-point function of planar maps and the loop–loop propagator of cylindrical maps. Our main results are explicit exact expressions for these correlators, already at a discrete level, in the particular case of quadrangulations. For quadrangulations of large area n, several regimes are obtained according to whether the boundary is small (with a length which remains finite), dense (with a length of order n) or critical (with a length of order $n^{1/2}$). We derive from our discrete results explicit expressions for the scaling limit of the bulk–boundary and boundary–boundary correlators in all these regimes. Most, but not all, of these scaling limits are universal and we recover in particular some results of [6] and [7], here via a rigorous discrete enumeration. Maps with a critical boundary are characterized by a one-parameter family of universal scaling functions, corresponding to a new probabilistic limiting object interpolating between the Brownian map and the Brownian continuum random tree. We first derive our expressions in the context of quadrangulations with *generic boundaries*, i.e. boundaries which may have 'pinch points' separating the map into several components. Our results for the bulk–boundary correlator are then extended, both at the discrete level and in the various continuous regimes, to the case of *self-avoiding boundaries* where pinch points on the boundary are forbidden. For large maps, generic and self-avoiding boundaries lead to the same scaling regimes. We finally address the problem of planar quadrangulations equipped with a self-avoiding loop. We give exact discrete and continuous expressions for the *bulk–loop correlator*, which is the law for the distance to the loop of a vertex drawn at random in the map. Here again, for large maps, a regime of critical self-avoiding loop is found, described by a new one-parameter family of scaling functions.

This paper is organized as follows. Section 2 presents our main results, which are then proved in sections 3–6. We give in section 2.1 a precise definition of quadrangulations with a boundary and present in section 2.2 a number of explicit discrete formulae for various generating functions encoding the bulk–boundary and boundary–boundary correlators. The cases of both generic and self-avoiding boundaries are discussed. We then turn in section 2.3 to the statistics of distances in large maps, for which several scaling regimes are found, depending on whether the boundary is small, dense or critical. We give in particular explicit expressions for various scaling functions characterizing these regimes. We finally discuss in section 2.4 the bulk–loop correlator for quadrangulations with a self-avoiding loop, both at the discrete and continuous levels. Section 3 gives a precise derivation of our results for quadrangulations with a generic boundary at the discrete level. We present in section 3.1 a bijection relating these quadrangulations to cyclic sequences of well-labeled trees. This property is used in section 3.2 to derive explicit formulae for associated generating functions. Physically, these correspond to the bulk–boundary and boundary–boundary correlators in a grand canonical ensemble with a boundary of fluctuating length, conjugate to a fugacity parameter z. We then deduce in section 3.3 the corresponding fixed-length generating functions, corresponding to an ensemble of quadrangulations with a boundary of fixed length. Section 4 is devoted to the scaling limit of large maps with a generic boundary. We analyze in section 4.1 the singularities of our discrete generating functions, which control the large map properties. Three different

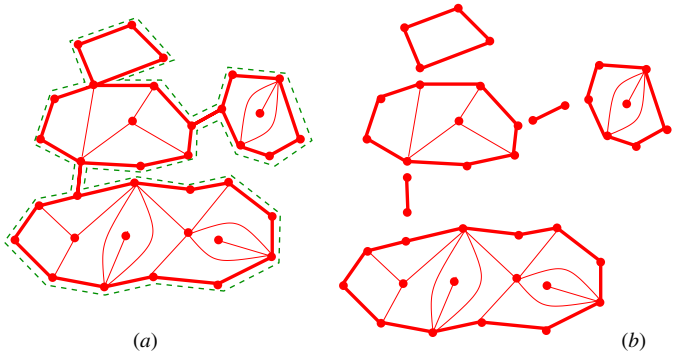

Figure 1. An example (a) of quadrangulation with a boundary of area $n = 17$ and perimeter $2p = 34$, which is the length of its contour (dashed green line). All faces are tetravalent, except for the external one which has degree $2p$. Upon splitting the boundary at its separating vertices, we obtain (b) irreducible components (here six) which are either single edges or quadrangulations with a self-avoiding boundary.

scaling regimes are found: a small boundary regime for $z < 1/8$, discussed in detail in section 4.2, a dense boundary regime for $z > 1/8$, discussed in detail in section 4.3, and finally a 'critical' regime for $z \sim 1/8$. This latter regime is best analyzed in section 4.4 in the fixed length ensemble by considering large quadrangulations whose boundary has a length proportional to the square root of their area. This gives rise to our one-parameter family of scaling functions. Section 5 deals with quadrangulations with a self-avoiding boundary. We first show in section 5.1 how to obtain an explicit formula for the corresponding bulk–boundary correlator from the expression of its generic boundary counterpart. This property is used in section 5.2 to analyze the large map scaling limit, which is shown to present essentially the same three scaling regimes as above. Finally, section 6 is devoted to quadrangulations with a self-avoiding loop. We show how to construct such quadrangulations by concatenating two quadrangulations with self-avoiding boundaries of the same length. This property is used to derive explicit expressions for the discrete and continuous bulk–loop correlators. In particular, a new family of scaling functions is found, describing maps with a critical self-avoiding loop. We end this paper by a few concluding remarks gathered in section 7.

2. Main results

This section presents a panorama of our results, which are listed without derivation. We will then explain in the following sections how those can be obtained.

2.1. Quadrangulations with a boundary: definitions

Here and throughout this paper, we define a *quadrangulation with a boundary* as a planar map with a distinguished face such that all the other faces of the map have degree 4. Such maps are sometimes called 'pseudo-quadrangulations' in the literature. We use the convention of representing the map in the plane with the point at infinity in the distinguished face (see figure 1), which we call the *external face* accordingly. Note that the degree of the external face is necessarily even.

We call the *boundary* of the quadrangulation the set of edges and vertices incident to the external face. The actual sequence of edges followed when going around the external face

counterclockwise in the plane is called the *contour*. The *perimeter* is the (even) length of this sequence, which is nothing but the degree of the external face. The *bulk* of the quadrangulation is the complement of the external face in the plane, and the number of *inner* faces it contains is called the *area*.

As in the usual terminology, a *pointed* map is a map with a marked vertex, which is referred to as the *origin*, while a *rooted* map is a map with a marked oriented edge, which is referred to as the *root edge*. Here, we will make the useful convention that a *rooted quadrangulation with a boundary* has always its root edge on the boundary, with the external face incident to its right. We also consider in the following maps which are both pointed and rooted, or maps with are doubly rooted, in which cases all root edges are boundary edges with the appropriate orientation.

Note that we consider here general maps which may possibly contain separating vertices or edges (a vertex or an edge is separating if its deletion disconnects the map). In particular, the boundary may contain such separating vertices or edges, which are those encountered several times along the contour. When the boundary has no separating vertices nor edges, it is said to be *self-avoiding*. Upon splitting at the separating vertices of the boundary, a quadrangulation with a *generic* boundary is naturally decomposed into several 'irreducible' components that are quadrangulations with a self-avoiding boundary or possibly single edges, arranged in a tree-like structure (see figure 1). This decomposition will later allow us to study quadrangulations with a self-avoiding boundary using results obtained for generic boundaries, which we present first.

2.2. Discrete results

We wish to enumerate quadrangulations with a (generic) boundary having prescribed area and perimeter. In the following, these two quantities will usually be denoted, respectively, by n and $2p$. As customary, the results are best expressed via a *generating function*, corresponding to a sum over all quadrangulations with a boundary, a given quadrangulation with area n and perimeter $2p$ having a contribution $g^n z^p$. We will thus consider power series in two variables g and z. Again, our results are here stated without derivation, which can be found in sections 3 (for generic boundaries) and 5 (for self-avoiding boundaries).

Arguably the simplest generating function is that for rooted quadrangulations with a boundary, already computed for instance in [24], and which may be written as

$$W_0 = W(1 - gR^2(W - 1)), \tag{2.1}$$

where R and W are the unique power series satisfying the algebraic equations

$$\begin{aligned} R &= 1 + 3gR^2 \\ W &= 1 + zRW^2. \end{aligned} \tag{2.2}$$

The particular form of this generating function yields, by two applications of the Lagrange inversion formula, an explicit expression for the number of rooted quadrangulations with a boundary having area n and perimeter $2p$:

$$W_0|_{g^n z^p} = \frac{3^n (2p)!}{p!(p-1)!} \frac{(2n+p-1)!}{n!(n+p+1)!}, \tag{2.3}$$

where $\cdot|_{g^n z^p}$ denotes the extraction of the coefficient of $g^n z^p$ in the series.

In this paper, we are interested in refined quantities involving the graph distance. Our main results are exact expressions for the bulk–boundary correlator and the boundary–boundary correlator which are defined as follows.

The *bulk–boundary correlator* is the generating function for pointed quadrangulations with a boundary, where the origin is at a prescribed distance, say d, from the boundary. It reads

$$G_d = \log\left(\frac{W_d}{W_{d-1}}\right), \tag{2.4}$$

where

$$W_d \equiv W\frac{1-(W-1)f_{d+1}}{1-(W-1)f_d}, \qquad f_d \equiv x\frac{(1-x^d)}{(1-x^{d+2})} \tag{2.5}$$

and x is the power series satisfying

$$x = gR^2(1+x+x^2). \tag{2.6}$$

A few remarks are in order. The maps considered here might have non-trivial symmetries, and the generating function G_d includes the corresponding usual inverse symmetry factor. W_d has itself a combinatorial interpretation, as the generating function for pointed rooted quadrangulations with a boundary, such that the origin is at distance *smaller than or equal to* d from the boundary, and such that the root edge starts from a (boundary) vertex closest to the origin. Such maps have no symmetries. Finally, the expression (2.1) is consistent with (2.5) for $d = 0$, while $W_d \to W$ for $d \to \infty$, so that W is the generating function for pointed rooted quadrangulations with a boundary.

The *boundary–boundary correlator* is the generating function for doubly rooted quadrangulations with a boundary, such that the two root edges start from (boundary) vertices at a distance d from each other in the map. It reads

$$T_d = W^2(W-1)^d f_1\left(\frac{1}{f_{d+1}} - 2(W-1) + f_{d+1}(W-1)^2\right). \tag{2.7}$$

No symmetry factors are involved.

Let us now consider quadrangulations with a self-avoiding boundary. A classical combinatorial argument shows that the generating function $\tilde{W}_0$ for rooted quadrangulations with a self-avoiding boundary is related to W_0 via

$$\tilde{W}_0(g,Z) = W_0(g,z) \qquad \text{with} \qquad Z = zW_0^2(g,z), \tag{2.8}$$

where we emphasize that $\tilde{W}_0$ is a power series in two variables g and Z, Z being the variable conjugated to the half-perimeter of the self-avoiding boundary and g still being conjugated to the area. Algebra yields

$$\tilde{W}_0 = \tilde{W}(1 - gR^2(\tilde{W}-1)), \tag{2.9}$$

where R is still given by (2.2) while $\tilde{W}$ obeys

$$\tilde{W} = 1 + ZR/(1-gR^2(\tilde{W}-1))^2. \tag{2.10}$$

By double Lagrange inversion we find the number of rooted quadrangulations with a self-avoiding boundary having area n and perimeter $2p$

$$\tilde{W}_0|_{g^n Z^p} = 3^{n-p}\frac{(3p)!}{p!(2p-1)!}\frac{(2n+p-1)!}{(n-p+1)!(n+2p)!}. \tag{2.11}$$

Note that for self-avoiding boundaries we have the constraint $1 \leqslant p \leqslant n+1$. The bulk–boundary correlator, defined in the same way as for generic boundaries, reads

$$\tilde{G}_d = \log\left(\frac{\tilde{W}_d - \tilde{W}_0 + 1}{\tilde{W}_{d-1} - \tilde{W}_0 + 1}\right) \qquad \text{for} \quad d \geqslant 1, \qquad \tilde{G}_0 = \tilde{W}_0 - 1, \tag{2.12}$$

where

$$\tilde{W}_d = \frac{\tilde{W}}{\tilde{W}_0} \times \frac{1-(\tilde{W}-1)f_{d+1}}{1-(\tilde{W}-1)f_d} + \tilde{W}_0 - 1. \tag{2.13}$$

Again the generating function $\tilde{G}_d$ involves symmetry factors, unlike $\tilde{W}_d$ which has the same combinatorial interpretation as W_d, now in the context of quadrangulations with a self-avoiding boundary. We have not been able to find a compact expression for the boundary–boundary correlator for self-avoiding boundaries.

2.3. Distance statistics in quadrangulations with a boundary

From these above exact expressions, we may now derive statistical information on distances in quadrangulations with a boundary. More precisely, we consider random quadrangulations with a boundary having prescribed area n and perimeter $2p$, where each sample map appears with a probability proportional to its inverse symmetry factor. We are particularly interested in the large n limit, for which we expect to find asymptotically the same results as with the uniform measure. Until further notice we consider generic (possibly non-self-avoiding) boundaries.

It proves convenient to consider first the *fixed z ensemble* where the area remains fixed equal to n but the perimeter fluctuates, and each sample map with perimeter $2p$ appears with probability proportional to z^p (besides the symmetry factor). This model is well defined (has a finite partition function for all n) for $0 \leqslant z \leqslant 1/4$. The above generating functions correspond to observables related to the distance. The bulk–boundary correlator encodes the distance between the boundary and a random vertex uniformly drawn in the bulk. The probability that this *bulk–boundary distance* be d is $(G_d|_{g^n})/(\log W|_{g^n})$, while the probability that it be less than or equal to d is nothing but $(\log W_d|_{g^n})/(\log W|_{g^n})$. The boundary–boundary correlator encodes the distance between (the origins of) two edges uniformly chosen on the boundary. The probability that this *boundary–boundary distance* be d is $(T_d|_{g^n})/\big(2z\frac{\mathrm{d}}{\mathrm{d}z}W_0|_{g^n}\big)$.

For $n \to \infty$, the model exhibits a phase transition at $z = 1/8$, which might be seen simply by analyzing W_0:

- when $z < 1/8$ (*subcritical regime*), the perimeter remains finite as $n \to \infty$,
- when $z > 1/8$ (*supercritical regime*), the perimeter is of order n and, up to Gaussian fluctuations of order $n^{1/2}$, it concentrates around its mean value $2\langle p\rangle_n(z)$ with

$$\langle p\rangle_n(z) \sim n\frac{8z-1}{1-4z}, \tag{2.14}$$

- when $z \sim 1/8$ (*critical regime*), the perimeter is of order $n^{1/2}$.

We will be especially interested in the critical regime, and for this case only we will perform the translation back to the fixed perimeter ensemble, considering quadrangulations with a boundary having fixed (large) area n and (large) perimeter $2p$, keeping the renormalized half-perimeter $P \equiv p \cdot n^{-1/2}$ finite. Let us now discuss the manifestations of the transition on the distance statistics, as seen by analyzing G_d and T_d. Table 1 gives a qualitative summary of the asymptotic behavior for the perimeter, the bulk–boundary distance and the boundary–boundary distance in the various regimes.

In the subcritical regime, the bulk–boundary distance is of order $n^{1/4}$ and admits a continuous limit law which does not depend on z (provided that it is in the subcritical range $]0, 1/8[$), and whose (cumulative) distribution function reads

$$\Phi(D) \equiv \lim_{n\to\infty} \frac{\log W_{\lfloor Dn^{1/4}\rfloor}|_{g^n}}{\log W|_{g^n}} = \frac{2}{\sqrt{\pi}}\int_{-\infty}^{\infty} \mathrm{d}\xi\, \mathrm{i}\xi\, \mathrm{e}^{-\xi^2}\mathcal{F}(D; -\xi^2), \tag{2.15}$$

Table 1. Scaling behavior of the perimeter; the bulk–boundary distance and the boundary–boundary distance, when the area n becomes large while z is fixed, for the three different regimes.

	Perimeter	Bulk–boundary distance	Boundary–boundary distance	Universality class
$z < 1/8$	Finite	$n^{1/4}$	Finite	Brownian map
$z > 1/8$	n	Finite	$n^{1/2}$	Brownian CRT
$z \sim 1/8$	$n^{1/2}$	$n^{1/4}$	$n^{1/4}$	Brownian map with a boundary

where

$$\mathcal{F}(D;\mu) \equiv \sqrt{\mu}\left(1+\frac{3}{\sinh^2\left(\sqrt{\frac{3}{2}}\,\mu^{1/4}D\right)}\right). \tag{2.16}$$

We recognize the universal two-point function of pure 2D gravity [6, 7] also obtained in the case of quadrangulations without a boundary [12]. This result agrees with the physical intuition: upon rescaling distances by a factor $n^{-1/4}$, the boundary reduces to a point which behaves no different from a typical point in a large random quadrangulation. Mathematically, the metric space obtained in the scaling limit is expected to be the Brownian map. In contrast, the boundary–boundary distance remains finite and admits a non-universal discrete limit law with a computable, albeit complicated, expression.

In the supercritical regime, the bulk–boundary distance remains finite at large n and admits a non-universal discrete limit law, whose cumulative distribution function reads

$$\phi_z(d) \equiv \lim_{n\to\infty} \frac{\log W_d|_{g^n}}{\log W|_{g^n}} = \frac{(1-(x_{\rm crit}(z))^{d+1})(1-(x_{\rm crit}(z))^{d+2})}{(1+(x_{\rm crit}(z))^{d+1})(1+(x_{\rm crit}(z))^{d+2})}, \tag{2.17}$$

where

$$x_{\rm crit}(z) \equiv \frac{16z-1-\sqrt{3((8z)^2-1)}}{2(1-4z)}. \tag{2.18}$$

The boundary–boundary distance is of order $n^{1/2}$ and admits a continuous limit law. Using the square root of the mean half-perimeter (2.14) as a distance unit, we find the Rayleigh probability density function

$$\tilde{\rho}_{\rm bound.}(\delta) \equiv \lim_{n\to\infty}\left(\frac{T_{\lfloor\delta\cdot\sqrt{\langle p\rangle_n(z)}\rfloor}|_{g^n}}{2z\frac{d}{dz}W_0|_{g^n}}\cdot\sqrt{\langle p\rangle_n(z)}\right) = 2\delta\,\mathrm{e}^{-\delta^2}, \tag{2.19}$$

which coincides with the two-point function for the Brownian continuum random tree [25]. The (Brownian) CRT is expected to be the limiting metric space obtained when rescaling distances by a factor $n^{-1/2}$. The physical interpretation is that, in the supercritical phase, the boundary becomes 'dense' in the quadrangulation and folds onto itself, creating a branched structure.

In the critical regime, both the bulk–boundary and boundary–boundary distances are of order $n^{1/4}$. Both admit continuous limit laws, which are best expressed in the (critical) fixed perimeter ensemble. On the one hand, the bulk–boundary distance cumulative distribution function reads

$$\begin{aligned}\bar{\Phi}(D,P) &\equiv \lim_{n\to\infty,\,p\sim Pn^{1/2}} \frac{\log W_{\lfloor Dn^{1/4}\rfloor}\big|_{g^n z^p}}{\log W|_{g^n z^p}} \\ &= 2\sqrt{P}\,\mathrm{e}^{P^2/4}\int_{-\infty}^{\infty}\mathrm{d}\xi\,\frac{\xi}{\mathrm{i}}\,\mathrm{e}^{-\xi^2}\bar{\mathcal{H}}(D,P;-\xi^2),\end{aligned} \tag{2.20}$$

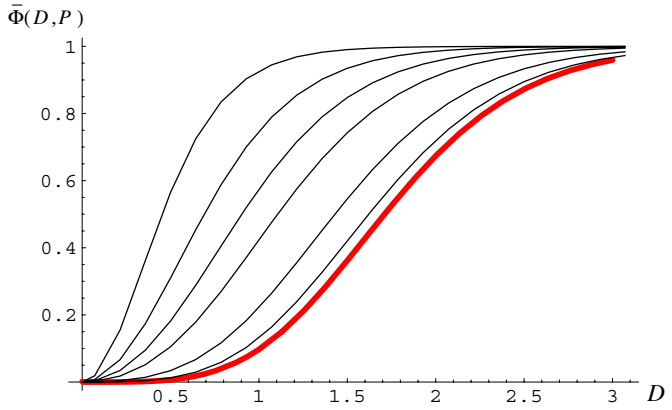

Figure 2. Plots of the cumulative distribution function $\bar\Phi(D,\,P)$ as a function of D, for $P = 0.01$, 0.1, 0.5, 1.0, 2.0 and 5.0 (thin lines from bottom to top). We also indicate (thick red line) the (integrated) two-point function $\Phi(D)$.

where

$$\bar{\mathcal{H}}(D,\,P;\,\mu) \equiv \frac{\mathrm{e}^{-\sqrt{\mu}P}}{\sqrt{\pi}\,P^{3/2}}\left\{1+\left(3\sqrt{\mu}-2f^2(D;\,\mu)\right)\int_0^\infty \mathrm{d}K\,\mathrm{e}^{-\frac{K^2}{P}-2f(D;\mu)K}\,2K\right\}$$
$$f(D;\,\mu) \equiv \sqrt{\frac{3}{2}}\,\mu^{1/4}\coth\left(\sqrt{\frac{3}{2}}\,\mu^{1/4}D\right). \tag{2.21}$$

It is plotted in figure 2 as a function of D, for $P = 0.01$, 0.1, 0.5, 1.0, 2.0 and 5.0. As we will show later, for $P \to 0$ we recover the two-point function $\Phi(D)$ (shown in red on figure 2), while for $P \to \infty$ the rescaled bulk–boundary distance is of order $P^{-1/2}$ and $\bar\Phi(D,\,P)$ takes the simple scaling form

$$\bar\Phi(D,\,P) \sim \tanh^2\left(\tfrac{\sqrt{3}}{2}D\sqrt{P}\right) \tag{2.22}$$

consistent with the supercritical law (2.17) for $z \to 1/8^+$. On the other hand, the boundary–boundary distance probability density function reads

$$\begin{aligned}\bar\rho_{\text{bound.}}(D,\,P) &\equiv \lim_{n\to\infty,\,p\sim Pn^{1/2}}\left(\frac{T_{\lfloor Dn^{1/4}\rfloor}\big|_{g^n z^p}}{2z\,\frac{d}{dz}W_0\big|_{g^n z^p}}\cdot n^{1/4}\right)\\ &= \frac{4}{3P^4}\,\mathrm{e}^{-D^2/P}\{(2D^3-3DP)+(4D^2P-2P^2)\sigma_1(D,\,P)+2DP^2\sigma_2(D,\,P)\},\end{aligned} \tag{2.23}$$

where

$$\begin{aligned}\sigma_1(D,\,P) &= \frac{2\,\mathrm{e}^{P^2/4}}{\sqrt{\pi}P}\int_{-\infty}^{\infty}\mathrm{d}\xi\,\frac{\xi}{\mathrm{i}}\,\mathrm{e}^{-\xi^2+\mathrm{i}\xi P}f(D;\,-\xi^2)\\ \sigma_2(D,\,P) &= \frac{2\,\mathrm{e}^{P^2/4}}{\sqrt{\pi}P}\int_{-\infty}^{\infty}\mathrm{d}\xi\,\frac{\xi}{\mathrm{i}}\,\mathrm{e}^{-\xi^2+\mathrm{i}\xi P}f^2(D;\,-\xi^2)\end{aligned} \tag{2.24}$$

and $f(D,\,\mu)$ is given by (2.21). It is also natural to measure the boundary–boundary distance in units of $\sqrt{p}$ which amounts to introducing the variable $\delta = D/\sqrt{P}$. The corresponding probability density $\tilde\rho_{\text{bound.}}(\delta,\,P)$ is plotted in figure 3 for $P = 0.5$, 1.0, 1.5, 2.0, 3.0, 5.0, 10.0.

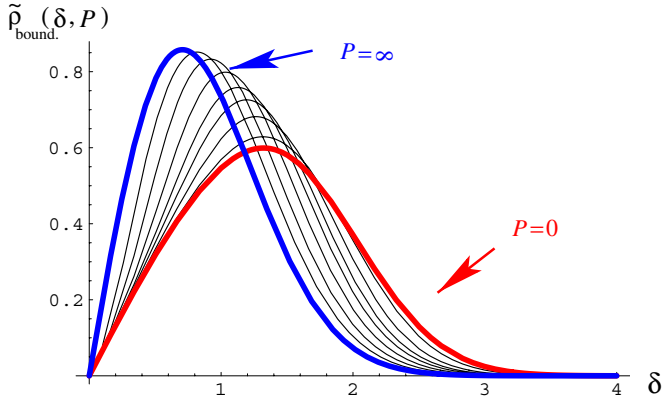

Figure 3. Plots of the probability density $\tilde{\rho}_{\text{bound.}}(\delta, P)$ as a function of the rescaled distance $\delta = D/\sqrt{P}$ for $P = 0.5, 1.0, 1.5, 2.0, 3.0, 5.0, 10.0$ (thin lines from bottom to top). We also indicate the Rayleigh law of equation (2.19) (upper blue thick line) corresponding to the limit $P \to \infty$ and the non-trivial law of equation (2.25) (lower red thick line) corresponding to the limit $P \to 0$.

When $P \to \infty$ we precisely recover the Rayleigh density (2.19), while for $P \to 0$ we have the particularly simple but non-trivial expression:

$$\tilde{\rho}_{\text{bound.}}(\delta, P) \overset{P\to 0}{\to} \frac{2}{105} \mathrm{e}^{-\delta^2}(35\delta + 28\delta^3 + 12\delta^5 + 3\delta^7). \tag{2.25}$$

We emphasize that all these expressions are expected to be universal (up to a possible rescaling of the distance and perimeter) and are intrinsic to the metric space obtained in the scaling limit. More precisely, up to a change of the distance scale, we have a one-parameter family of random metric spaces indexed by the (renormalized) perimeter P. It might be called the *Brownian map with a boundary*. Note that P is not homogeneous to a distance but to its square, an indication that the fractal dimension of the boundary is 2. The Brownian map with a boundary interpolates smoothly between the Brownian map, recovered for $P = 0$, and the Brownian continuum random tree, recovered in the limit $P \to \infty$. Note that when $P \to 0$, we observe a deviation from the Brownian map statistics for small distances of order $\sqrt{P}$ (corresponding to finite values of δ above).

Let us now briefly mention the results for quadrangulations with a self-avoiding boundary. Observe that the generating functions $\tilde{W}_0$ and $\tilde{G}_d$ are related to random quadrangulations with a self-avoiding boundary in exactly the same way as W_0 and G_d are related to random quadrangulations with a generic boundary. A parallel approach can thus be followed. Here Z denotes the activity per unit of half-perimeter. There is now a phase transition at $Z = 2/9$ which is expected to be in the same universality class as the above. From the exact expressions for $\tilde{W}_0$ and $\tilde{G}_d$ we can show that

- for $Z < 2/9$, the perimeter remains finite as the area n tends to infinity, while the bulk–boundary distance is of order $n^{1/4}$ with the same limit law (2.15),
- for $Z > 2/9$, the perimeter is of order n and concentrates around its non-universal mean value, while the bulk–boundary distance is finite and has a non-universal discrete limit law,
- for $Z \sim 2/9$, the perimeter is of order $n^{1/2}$, while the bulk–boundary distance is of order $n^{1/4}$.

In this latter case, we may as well consider the critical fixed perimeter ensemble and compute the bulk–boundary distance cumulative distribution function. We find the same expression as in (2.20) up to a factor of 3 in the renormalized perimeter P (see details in section 5.2). This is a first non-trivial check of the universality of our analytical expressions.

2.4. Application to self-avoiding loops

Another interesting application of our exact discrete results is that they allow us to study the statistics of distances in *quadrangulations with a self-avoiding loop*. More precisely, a self-avoiding loop is a closed path made of consecutive edges of the quadrangulation, which is *simple*, i.e. visits any vertex at most once. We consider planar quadrangulations with a distinguished oriented self-avoiding loop (and no boundary: all faces have degree 4). The area is the total number of faces, while the loop length is necessarily even. Again we consider a statistical model where the area n is fixed, where the loop length $2p$ may either be fixed or be controlled by a weight y^p, and where in all rigor we need to incorporate the inverse symmetry factor, irrelevant for $n \to \infty$. This is a particular instance of the so-called $\mathbf{O}(\mathcal{N} = 0)$ model on a random lattice, slightly different from those studied with matrix model techniques [26] where the loops would run on the dual map.

The connection with quadrangulations with a boundary is easily seen. Upon cutting along the loop, a quadrangulation with a self-avoiding loop yields two quadrangulations with a self-avoiding boundary, constrained to have the same perimeter. The orientation of the loop allows us to distinguish these two pieces as left and right, and we clearly have a bijection preserving the total area. We can therefore express a number of generating functions for this problem in terms of the generating functions found above. For instance, the generating function for quadrangulations with a self-avoiding loop and a marked vertex on the loop reads

$$\Gamma_0(g, y) = \sum_{p \geqslant 1} y^p (\tilde{W}_0(g, Z)|_{Z^p})^2, \tag{2.26}$$

where g is the weight per face while $\sqrt{y}$ is the weight per edge of the loop. More generally, we may consider the generating function for quadrangulations with a self-avoiding loop and a marked vertex at distance d from the loop and lying on its right. It reads

$$\Gamma_d(g, y) = \sum_{p \geqslant 1} y^p \tilde{W}_0(g, Z)|_{Z^p} \tilde{G}_d(g, Z)|_{Z^p} \tag{2.27}$$

if the configurations are counted with their inverse symmetry factor. Constraining the marked vertex to be on the right of the loop ensures that both expressions are consistent for $d = 0$, and by symmetry it causes no loss of generality. Statistically, Γ_d encodes the *bulk–loop distance*, i.e. the distance between the loop and a random vertex uniformly drawn in the bulk. In the following sections, we provide more explicit (yet slightly involved) expressions for $\tilde{W}_0|_{Z^p}$ and $\tilde{G}_d|_{Z^p}$, easing the task of deducing the bulk–loop distance statistics for maps of large fixed size n. To sum up our results, we find a phase transition at $y = 4/81$.

- For $y < 4/81$, the loop length remains finite as $n \to \infty$, and the bulk–loop distance is of order $n^{1/4}$ with a distribution again characterized by the two-point function (2.15). The physical interpretation is that the loop remains microscopic and is thus irrelevant in the scaling limit, where distances are rescaled by a factor $n^{-1/4}$, and which is still described by the Brownian map.
- For $y > 4/81$, the loop length is of order n and the bulk–loop distance is finite. The physical interpretation is that the loop becomes dense in the quadrangulation. We however lack evidence that the scaling limit (on a scale $n^{1/2}$) is still described by the Brownian CRT, though this hypothesis is plausible.

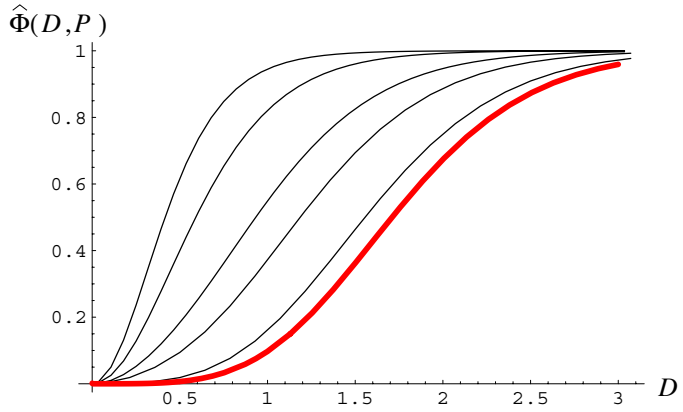

Figure 4. The cumulative distribution function $\hat{\Phi}(D, P)$ as a function of the bulk–loop distance for a self-avoiding loop of (rescaled) half-length $P = 0.01$, 0.1, 0.2, 0.5 and 1.0 (thin lines from bottom to top). We also indicated (thick red line) the limiting two-point function $\Phi(D)$.

– For $y \sim 4/81$, the loop length is of order $n^{1/2}$ and the bulk–loop distance is of order $n^{1/4}$.

Here again we are most interested in this critical case, and the results are best expressed in the ensemble where both the area n and the loop length $2p$ are prescribed, and jointly taken to be large keeping the ratio $P = p \cdot n^{-1/2}$ finite. The scaling law for the bulk–loop distance cumulative distribution function reads

$$\hat{\Phi}(D, P) \equiv \lim_{n\to\infty, p\sim Pn^{1/2}} \frac{\sum_{k=0}^{\lfloor Dn^{1/4}\rfloor} \Gamma_k\big|_{g^n y^p}}{\sum_{k=0}^{\infty} \Gamma_k\big|_{g^n y^p}}$$
$$= \frac{18P^3\sqrt{\pi}}{1+18P^2}\, \mathrm{e}^{9P^2} \int_{-\infty}^{\infty} \mathrm{d}\xi\, \frac{\xi}{\mathrm{i}}\, \mathrm{e}^{-\xi^2}\, \hat{\mathcal{H}}(D, P; -\xi^2), \tag{2.28}$$

where

$$\hat{\mathcal{H}}(D, P; \mu) \equiv 3\frac{\mathrm{e}^{-6\sqrt{\mu}P}}{\pi(3P)^4}(1+3P\sqrt{\mu})$$
$$\times \left\{1+\left(3\sqrt{\mu}-2f^2(D;\mu)\right)\int_0^{\infty} \mathrm{d}K\, \mathrm{e}^{-\frac{K^2}{3P}-2f(D;\mu)K} 2K\right\}. \tag{2.29}$$

It is plotted in figure 4 for $P = 0.01$, 0.1, 0.2, 0.5 and 1.0. When $P \to 0$, $\hat{\Phi}(D, P) \to \Phi(D)$ as expected while, when $P \to \infty$, D is of order $P^{-1/2}$ and we have the scaling form

$$\hat{\Phi}(D, P) \sim \tanh^2\left(\sqrt{\tfrac{9}{2}} D\, \sqrt{P}\right). \tag{2.30}$$

The scaling function $\hat{\Phi}(D, P)$ is expected to be universal, and characteristic of a model of self-avoiding loop on a Brownian map.

3. Quadrangulations with a boundary: combinatorics

We now come to the derivation of the expressions given in section 2.2 for the various generating functions concerning quadrangulations with a generic boundary. Our approach is based on a bijection with simpler objects, namely sequences of well-labeled trees, as discussed just below.

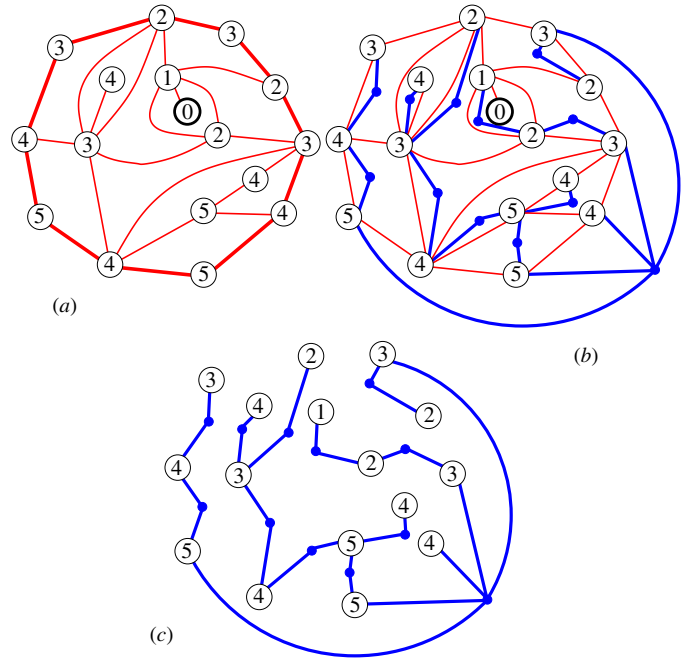

Figure 5. An example (*a*) of pointed quadrangulation with a boundary. We have labeled each vertex by its graph distance from the origin (vertex with label 0). Adding (*b*) to each face an unlabeled vertex and connecting it to those labeled vertices followed by a smaller label clockwise within the face, we end up (*c*) with a particular labeled mobile whose unlabeled vertices all have degree 2, except for that associated with the external face, which has a degree equal to half the perimeter of the quadrangulation. The labels around this vertex satisfy the property (P) of the text.

3.1. Bijection

A quadrangulation with a boundary is a particular instance of a bipartite planar map. As such, it may be coded by a so-called *well-labeled mobile*, as explained in section 2 of [10] (see figure 5). More precisely, the coding is for a pointed map (i.e. a map with a chosen origin vertex). The associated mobile is a plane tree with alternating labeled and unlabeled vertices. The labeled vertices correspond to the original vertices of the map and they carry an integer label equal to the graph distance in the map from the corresponding vertex to the origin. The unlabeled vertices of the mobile correspond to the faces of the map and their degree is half the degree of the corresponding face in the map. Around each unlabeled vertex v, we have the following property (P): reading the sequence of labels of vertices adjacent to v clockwise around v, any label ℓ is followed by a label larger than or equal to $\ell - 1$. Finally, the mobile has a minimum label equal to 1. For quadrangulations with a boundary of length $2p$, all the unlabeled vertices of the associated mobile necessarily have degree 2, except for that associated with the external face, which we call the *external vertex* and whose degree is p. Those bi-valent unlabeled vertices may be erased, giving rise to edges which connect the labeled vertices directly. The property (P) may then be rephrased into the property (P') that *labels on adjacent labeled vertices differ by at most 1*. The resulting object is therefore a collection of p *well-labeled trees*, i.e. trees with labeled vertices satisfying (P'), attached to the external vertex by their root vertices, whose clockwise sequence of labels satisfies (P)

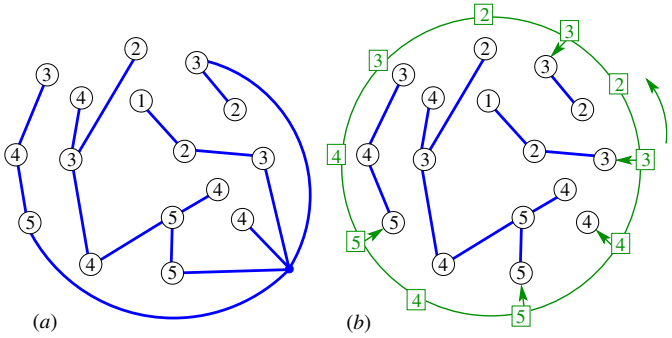

Figure 6. The well-labeled mobile of figure 5(*c*), where we erased the bi-valent unlabeled vertices (*a*), may alternatively be viewed (*b*) as a set of well-labeled trees satisfying the property (P') of the text, attached at each descending step of a (counterclockwise-oriented) cyclic sequence of integers (green outer circle) reproducing precisely the distance from the origin of the successive vertices along the contour of the quadrangulation (as apparent in figure 5(*a*)).

around the external vertex (see figure 6(*a*)). An equivalent but more convenient coding of the sequence of these p root labels around the external vertex is via a cyclic sequence of $2p$ non-negative integers such that consecutive integers differ by ± 1 (see figure 6(*b*)). In this coding, the root labels simply correspond to those integers which are followed immediately by a smaller integer in the cyclic sequence, and the property (P) is automatically satisfied. Moreover, the cyclic sequence of integers corresponds precisely to the distance to the origin of the successive boundary vertices along the contour (see figure 6(*b*)).

To summarize, we have a bijection between, on the one hand, pointed quadrangulations with a boundary and on the other hand cyclic sequences of non-negative integers such that consecutive integers differ but ± 1, with a well-labeled tree with root label ℓ attached to each descending step $\ell \to \ell - 1$ of the cyclic sequence, and with the requirement that the global minimum label be 1. Under this bijection, we have the following correspondences.

- The total number of edges for all the well-labeled trees is equal to the area n (the number of inner faces) of the quadrangulation.
- The label of any vertex is equal to the distance to the origin of the corresponding vertex on the map.
- The (even) length of the cyclic sequence is equal to the length $2p$ of the boundary.
- The successive integers in the cyclic sequence are equal to the distance to the origin of the successive boundary vertices along the contour. In particular, the smallest integer d in this cyclic sequence is the smallest distance found between the origin and a vertex of the boundary, i.e. the *distance from the origin to the boundary*.

We may transform the cyclic sequence of non-negative integers into a Dyck path ($0 = \ell_0, \ell_1, \ldots, \ell_{2p-1}, \ell_{2p} = 0$) by reading the sequence from one of its minima and subtracting d from all the integers (see figure 7). To each descending step $\ell_i \to \ell_i - 1$ is now attached a well-labeled tree with root label $\ell_i + d$. Note that the cyclic sequence may have several minima, and choosing a particular minimum amounts to marking a boundary edge $d \to d + 1$ with, say, the external face to the right.

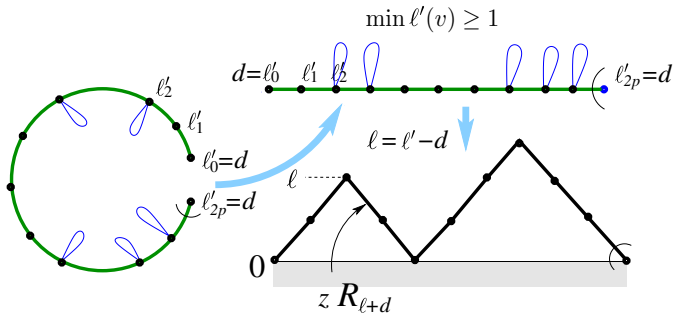

Figure 7. Opening a cyclic sequence of non-negative integers at one of its minima d results into a Dyck path ($0=\ell_0, \ell_1, \ldots, \ell_{2p-1}, \ell_{2p}=0$) by subtracting d from all integers in the sequence. To each descending step $\ell \to \ell-1$ of the Dyck path is attached a well-labeled tree with root label $\ell+d$, resulting in a weight $zR_{d+\ell}$ for the descending step if we demand that all the original labels be larger than 1.

3.2. Basic generating functions

We now wish to compute the generating function for pointed quadrangulations with a boundary, where a map with area n and perimeter $2p$ comes with a weight $g^n z^p$. Under the bijection, this weight simply amounts to a weight g per edge of the well-labeled trees and a weight z per descending step of the cyclic sequence of integers, or equivalently of the Dyck path.

A first ingredient is the generating function R_ℓ for rooted well-labeled trees with a root label $\ell \geqslant 1$ and with the condition that *all the labels on the tree be larger than or equal to 1*. This generating function was computed in [12] and reads

$$R_\ell = R\frac{[\ell]_x\ [\ell+3]_x}{[\ell+1]_x\ [\ell+2]_x}, \tag{3.1}$$

where we use the notation

$$[\ell]_x \equiv \frac{1-x^\ell}{1-x} \tag{3.2}$$

and where the quantities R and x are solutions of

$$R = 1+3gR^2, \qquad x = gR^2(1+x+x^2), \tag{3.3}$$

namely

$$\begin{aligned} R &= \frac{1-\sqrt{1-12g}}{6g}, \\ x &= \frac{1-24g-\sqrt{1-12g}+\sqrt{6}\sqrt{72g^2+6g+\sqrt{1-12g}-1}}{2(6g+\sqrt{1-12g}-1)}. \end{aligned} \tag{3.4}$$

We can now express the generating function W_d for Dyck paths with a well-labeled tree with root label ℓ_i+d attached at each descending step $\ell_i \to \ell_i-1$, and with a global minimum label larger than or equal to 1. This generating function reads

$$W_d = \sum_{p\geqslant 0} \sum_{\substack{\text{Dyck paths of length } 2p \\ (0=\ell_0,\ell_1,\ldots,\ell_{2p}=0)}} \prod_{\substack{\text{descending steps} \\ \ell_i\to\ell_i-1}} z\,R_{\ell_i+d} \tag{3.5}$$

with a conventional weight 1 for the trivial Dyck path of length 0. We have the recursion relation

$$W_d = 1+zR_{d+1}W_dW_{d+1}, \tag{3.6}$$

as obtained by decomposing any non-trivial Dyck path into its first ascending step $0 \to 1$, a path from 1 to 1 with all intermediate heights larger than or equal to 1 (weight W_{d+1} as obtained by a simple shift of labels), its first descending step $1 \to 0$ (weight zR_{d+1}) and a final Dyck path (weight W_d).

We may look for a solution of this equation in the form

$$W_d = W \frac{[d+2]_x}{[d+3]_x} \frac{V_{d+1}}{V_d}, \tag{3.7}$$

with W and V_d to be determined. Substituting this particular form in equation (3.6) leads to the equation

$$W\,[d+2]_x\,V_{d+1} = [d+3]_x\,V_d + zRW^2\,[d+1]_x\,V_{d+2}. \tag{3.8}$$

This relation is satisfied (for arbitrary R and x) upon taking

$$V_d = 1 + \lambda x^d \tag{3.9}$$

provided that we choose W and λ such that

$$\begin{aligned} W &= 1 + zRW^2 \\ W(-x^2 + \lambda x) &= (-x^3 + \lambda) + zRW^2(-x + \lambda x^2), \end{aligned} \tag{3.10}$$

namely

$$W = \frac{1 - \sqrt{1 - 4zR}}{2zR}, \qquad \lambda = x\frac{(W-1) - x}{1 - x(W-1)}. \tag{3.11}$$

Plugging this last expression back in (3.9) and (3.7), we end up with the desired solution

$$\begin{aligned} W_d &= W\,\frac{[d+2]_x}{[d+3]_x} \times \frac{[d+3]_x - x(W-1)\,[d+1]_x}{[d+2]_x - x(W-1)\,[d]_x} \\ &= W\,\frac{1 - (W-1)\,f_{d+1}}{1 - (W-1)\,f_d}, \end{aligned} \tag{3.12}$$

where W is explicitly given in terms of g and z as

$$W = \frac{3g - \sqrt{9g^2 - 6g(1 - \sqrt{1-12g})z}}{(1 - \sqrt{1-12g})z} \tag{3.13}$$

while we introduce the compact notation

$$f_d \equiv x\frac{[d]_x}{[d+2]_x} \tag{3.14}$$

with $[\cdot]_x$ defined above. In particular, we have $f_0 = 0$ and $f_1 = gR^2$. Note that W_d depends on the variable z only through the quantity W. In particular, for $d = 0$, we find

$$W_0 = W(1 - g\,R^2(W-1)) \tag{3.15}$$

which agrees with the known generating function for rooted pseudo-quadrangulations [24].

To go from Dyck paths back to cyclic sequences of integers, we simply have to identify the Dyck paths differing only by the choice of an instance of the smallest integer in the sequence. We note that equation (3.6) may be alternatively written as

$$W_d = \sum_{k \geqslant 0} (zR_{d+1}W_{d+1})^k, \tag{3.16}$$

where $(zR_{d+1}W_{d+1})^k$ is nothing but the generating function for Dyck paths with exactly k returns to 0. Cyclic sequences are then enumerated by

$$\sum_{k \geqslant 1} \frac{1}{k} (zR_{d+1}W_{d+1})^k = \log W_d, \tag{3.17}$$

where we use the convention of counting configurations with an inverse symmetry factor. A given configuration made of a cyclic sequence with its attached trees may only have a cyclic symmetry group $\mathbf{Z}_m$ (with m being a divisor of the number of minima k), and is then counted with a weight $1/m$.

So far, in the configurations counted by $\log W_d$, we imposed only that the global minimum label be larger than or equal to 1. To impose that this minimum label be exactly 1, as required by the bijection, we must suppress those configurations with a minimum larger than or equal to 2, whose generating function is obtained from the previous one by a simple shift of all labels by -1, i.e. is given by $\log W_{d-1}$. In particular, we deduce that the generating function G_d for quadrangulations with a boundary and a marked vertex at distance d from the boundary is simply given by

$$G_d = \log\left(\frac{W_d}{W_{d-1}}\right). \tag{3.18}$$

Again, configurations with an m-fold symmetry around the marked vertex are counted with a factor $1/m$.

As for the original quantity W_d, it is the generating function for quadrangulations with a boundary, with a marked vertex at a distance less than or equal to d from the boundary (the origin) and with a marked 'closest edge' to this origin, i.e. a boundary edge incident to a vertex at distance d from the origin and oriented counterclockwise around the bulk of the quadrangulation. Note that such pointed rooted maps cannot have any non-trivial symmetry. Finally, we may also interpret $\log W_d$ as the generating function for pointed quadrangulations with a boundary whose origin is at a distance less than or equal to d from the boundary.

As discussed in section 2, we are also interested in the generating function T_d for quadrangulations with a boundary having *two marked* (and distinguished) *boundary edges* oriented, say counterclockwise around the bulk of the quadrangulation, such that the origins of these marked edges are at a mutual distance d on the map. Taking the origin of the first marked edge as the origin of the map, we get under the bijection a cyclic sequence of integers with minimal value 0. The first marked edge defines a first step $0 \to 1$ at which we may start reading the cyclic sequence, leading to a Dyck path with a well-labeled tree with root label ℓ_i attached to each descending step $\ell_i \to \ell_i - 1$. Marking the second boundary edge amounts to choosing a step $d \to d \pm 1$ in the sequence, i.e. to choosing a point of height d in the Dyck path (for $d = 0$, this point must be different from the last one). Upon decomposing the Dyck path into a first ascending part from 0 to the marked point d and a second descending step from d to 0, we get the expression

$$\begin{aligned} T_d &= W_0 W_1 \cdots W_d \times (W_d z R_d)(W_{d-1} z R_{d-1}) \cdots (W_1 z R_1) W_0 \\ &= (W_0 W_1 \cdots W_d)^2 z^d (R_1 R_2 \cdots R_d), \end{aligned} \tag{3.19}$$

valid for $d > 0$. For $d = 0$, the actual decomposition yields $T_0 = W_0^2 - W_0$. From now on, we will assume $d > 0$ when referring to T_d. Upon substituting the expression (3.12) for W_d, we get

$$\begin{aligned} T_d &= W^2 (W-1)^d \frac{[1]_x}{[3]_x} \frac{([d+3]_x - x(W-1)\,[d+1]_x)^2}{[d+1]_x\,[d+3]_x} \\ &= W^2 (W-1)^d f_1 \left(\frac{1}{f_{d+1}} - 2(W-1) + f_{d+1}(W-1)^2\right). \end{aligned} \tag{3.20}$$

3.3. Fixed length generating functions

As we have already noticed, the quantities W_d and T_d depend on z only via the quantity W as given by equation (3.10), which we may rewrite as

$$z = \frac{w}{R\,(1+w)^2} \tag{3.21}$$

upon introducing the notation

$$w \equiv W - 1. \tag{3.22}$$

In this respect, W_d and T_d are the so-called Lagrangean generating functions, i.e. for which we can apply the Lagrange inversion theorem [27]. This means that we may extract an explicit expression for the z^p term of these generating functions. More precisely, the z^p term expressed as a contour integral in the variable z around 0 may be transformed by the change of variable $z \to w$ into a contour integral around 0 of the variable w, namely

$$\oint \frac{\mathrm{d}z}{2\mathrm{i}\pi} \frac{1}{z^{p+1}}\{\cdot\} = R^p \oint \frac{\mathrm{d}w}{2\mathrm{i}\pi} \frac{1}{w^{p+1}}(1-w)(1+w)^{2p-1}\{\cdot\}. \tag{3.23}$$

Upon expanding (3.12) in $w = W - 1$, we get the expression

$$W_d = (1+w)\left(1 - w\,(f_{d+1} - f_d) \sum_{k\geqslant 1} (w\,f_d)^{k-1}\right). \tag{3.24}$$

Taking the contour integral (3.23) of this quantity, we immediately get

$$\begin{aligned} W_d|_{z^p} &= R^p \left\{ \binom{2p}{p} - \binom{2p}{p-1} - (f_{d+1}-f_d) \sum_{k\geqslant 1} \left(\binom{2p}{p-k} - \binom{2p}{p-1-k} \right) (f_d)^{k-1} \right\} \\ &= R^p \left\{ \frac{(2p)!}{p!(p+1)!} - (f_{d+1}-f_d) \sum_{k=1}^{p} \frac{(2p)!}{(p-k)!(p+k+1)!} (2k+1)(f_d)^{k-1} \right\}. \end{aligned} \tag{3.25}$$

By a similar calculation, we easily obtain

$$(\log W_d)|_{z^p} = R^p \left\{ \frac{(2p-1)!}{(p!)^2} - 2 \sum_{k=1}^{p} \frac{(2p-1)!}{(p-k)!(p+k)!} \left((f_{d+1})^k - (f_d)^k \right) \right\} \tag{3.26}$$

for $p \geqslant 1$. For $d = 0$, we get in particular

$$W_0|_{z^p} = R^p \frac{(2p)!}{p!(p+2)!}(p + 2 - 3pf_1) = R^p \frac{(2p)!}{p!(p+2)!}\,(2 + p\,(2-R)) \tag{3.27}$$

with R given by (3.4). A second application of the Lagrange inversion formula, now for the variable g, yields

$$W_0|_{g^n z^p} = \frac{3^n (2p)!}{p!(p-1)!} \frac{(2n+p-1)!}{n!(n+p+1)!} \tag{3.28}$$

for $p \geqslant 1$. On the other hand, for $d \to \infty$, we have $W_d \to W$, with

$$W|_{z^p} = R^p \frac{(2p)!}{p!(p+1)!} \tag{3.29}$$

so that

$$W|_{g^n z^p} = \frac{3^n (2p)!}{(p-1)!(p+1)!} \frac{(2n+p-1)!}{n!(n+p)!} \tag{3.30}$$

for $p \geqslant 1$. The quantity $W_0|_{g^n z^p}$ is the number of quadrangulations with area n and boundary of length $2p$, where we have marked one of the $2p$ boundary edges on the contour. The

quantity $W|_{g^n z^p}$ is the number of the same quadrangulations with additional markings of one of their $n+p+1$ vertices (at some arbitrary distance from the boundary) as well as of a particular boundary edge closest to this vertex. The quantity

$$\frac{W|_{g^n z^p}}{W_0|_{g^n z^p}} \frac{2p}{n+p+1} = \frac{2p}{p+1} \tag{3.31}$$

measures therefore the average number of boundary edges closest to a uniformly chosen random vertex, for the ensemble of quadrangulations with area n and perimeter $2p$. Note that, surprisingly, this average number is independent of n (and its value thus matches that obtained for $n=0$, where quadrangulations with a boundary reduce to plane trees with p edges).

Finally, we may write (3.32) as

$$T_d = (1+w)^2 f_1 \left(\frac{w^d}{f_{d+1}} - 2w^{d+1} + w^{d+2} f_{d+1} \right) \tag{3.32}$$

so that we get

$$\begin{aligned} T_d|_{z^p} &= R^p f_1 \left\{ \frac{1}{f_{d+1}} \left(\binom{2p+1}{p-d} - \binom{2p+1}{p-1-d} \right) \right. \\ &\quad \left. - 2\left(\binom{2p+1}{p-1-d} - \binom{2p+1}{p-2-d} \right) + f_{d+1} \left(\binom{2p+1}{p-2-d} - \binom{2p+1}{p-3-d} \right) \right\} \\ &= 2R^p f_1 \left\{ \frac{(d+1)}{f_{d+1}} \frac{(2p+1)!}{(p-d)!(p+d+2)!} \right. \\ &\quad \left. - 2(d+2) \frac{(2p+1)!}{(p-d-1)!(p+d+3)!} + (d+3) f_{d+1} \frac{(2p+1)!}{(p-d-2)!(p+d+4)!} \right\}. \end{aligned} \tag{3.33}$$

By a slight refinement of this calculation, we can compute the generating function $T_d(s,s')$ for quadrangulations with a boundary of length $2p = s+s'$ with two marked boundary edges whose origins are separated by s steps counterclockwise along the contour and s' steps clockwise, and are at a mutual distance d on the map. We find

$$\begin{aligned} T_d(s;s') = R^{s+s'} f_1 \left\{ \frac{1}{f_{d+1}} C(s,d)C(s',d) - C(s,d)C(s',d+2) \right. \\ \left. - C(s,d+2)C(s',d) + f_{d+1} C(s,d+2)C(s',d+2) \right\}, \end{aligned} \tag{3.34}$$

where

$$C(s,d) \equiv \binom{s}{\frac{s-d}{2}} - \binom{s}{\frac{s-d}{2}-1}. \tag{3.35}$$

This result holds when d, s and s' have the same parity, while $T_d(s,s')$ vanishes otherwise.

4. Quadrangulations with a boundary: asymptotics

4.1. Critical lines

In order to describe the statistics of distances in large quadrangulations, we have to analyze the singular behavior of the various generating functions above. More precisely, the asymptotics for a large area n is encoded in the singularity reached at the radius of convergence in g of these generating functions. It is simpler to work first with a *fixed value of* z, corresponding to the fixed z ensemble mentioned in section 2. A first singularity is associated with the singular behavior of R and x, as given by equations (3.3) or (3.4), when g approaches the critical value

$$g_{\rm crit}^{(1)} = \tfrac{1}{12} \tag{4.1}$$

irrespectively of the value of z. This is the dominant singularity for $z < 1/8$ while, for $z \geqslant 1/8$, another singularity comes from the singular behavior of W, as given by equations (3.10) or (3.11), when zR approaches the value $1/4$, which defines the critical line

$$g^{(2)}_{\rm crit}(z) = \tfrac{1}{3}\, 4z\,(1-4z) \quad (z \geqslant 1/8). \tag{4.2}$$

Since $g^{(2)}_{\rm crit}(z) \leqslant 1/12$, this second singularity is dominant (i.e. determines the radius of convergence) whenever $z > 1/8$.

The radius of convergence therefore changes determination at

$$z_{\rm crit} = \tfrac{1}{8}. \tag{4.3}$$

As we shall see below, the generating functions have very different scaling behavior when z is smaller or larger than $z_{\rm crit}$. As discussed in section 2, this is the manifestation of a drastic change in the geometry of large quadrangulations with a boundary at this critical value.

4.2. Scaling limit: the $z < 1/8$ regime

Let us first discuss the case $z < 1/8$ for which the generating functions have radius of convergence $g^{(1)}_{\rm crit} = 1/12$. We may analyze the associated singularity by setting

$$g = \tfrac{1}{12}(1-\mu\epsilon) \tag{4.4}$$

with $\epsilon \to 0$. A sensible scaling limit for W_d is obtained by considering large distances of the form

$$d = D\,\epsilon^{-1/4}, \tag{4.5}$$

with D finite. We then have the following small ϵ expansions:

$$\begin{aligned} f_d &= 1 - 2f(D;\mu)\,\epsilon^{1/4} + (4f^2(D;\mu) - 3\sqrt{\mu})\,\epsilon^{1/2} + \cdots \\ f_{d+1} &= 1 - 2f(D;\mu)\,\epsilon^{1/4} + (6f^2(D;\mu) - 6\sqrt{\mu})\,\epsilon^{1/2} + \cdots, \end{aligned} \tag{4.6}$$

where we define

$$f(D;\mu) \equiv \sqrt{\tfrac{3}{2}}\,\mu^{1/4}\,\coth\left(\sqrt{\tfrac{3}{2}}\,\mu^{1/4} D\right). \tag{4.7}$$

We also have the expansion

$$W = A(z) - z\,A'(z)\,\sqrt{\mu}\,\epsilon^{1/2} + \cdots, \tag{4.8}$$

where we define

$$A(z) = \frac{1-\sqrt{1-8z}}{4z}. \tag{4.9}$$

Plugging these expressions in (3.12), we obtain the expansion

$$W_d = A(z) - \mathcal{F}(D;\mu)\,z\,A'(z)\,\epsilon^{1/2} + \cdots, \tag{4.10}$$

where we introduce the notation

$$\mathcal{F}(D;\mu) \equiv 2(f^2(D;\mu) - \sqrt{\mu}) = \sqrt{\mu}\left(1 + \frac{3}{\sinh^2\left(\sqrt{\tfrac{3}{2}}\,\mu^{1/4} D\right)}\right). \tag{4.11}$$

We may alternatively derive (4.10) by using the explicit form (3.25) of $W_d|_{z^p}$ and expanding it at small ϵ. Using the expansion

$$R = 2(1 - \sqrt{\mu}\,\epsilon^{1/2} + \cdots), \tag{4.12}$$

we obtain that

$$W_d|_{z^p} = 2^p \left\{ \frac{(2p)!}{p!(p+1)!} - \sqrt{\mu}\,\epsilon^{1/2} \frac{(2p)!}{(p-1)!(p+1)!} \right.$$
$$\left. -(2f^2(D;\mu)-3\sqrt{\mu})\,\epsilon^{1/2} \sum_{k=1}^{p} \frac{(2p)!}{(p-k)!(p+k+1)!}(2k+1) \right\} + \cdots$$
$$= 2^p \frac{(2p)!}{p!(p+1)!} \left\{ 1 - p\,\mathcal{F}(D;\mu)\,\epsilon^{1/2} + \cdots \right\}. \tag{4.13}$$

Upon summing over p with a weight z^p, this reproduces precisely the expression (4.10). Note that the 'kernel' $\mathcal{F}(D;\mu)$ occurring in (4.13) is independent of p. For $p = 1$, quadrangulations with a boundary of length 2 are equivalent, upon closing the boundary, to *rooted quadrangulations*, i.e. quadrangulations with a marked edge. The kernel $\mathcal{F}(D;\mu)$ is therefore the same as that encountered in [12] when deriving the continuous two-point function of planar quadrangulations from the generating function of rooted quadrangulations.

We may repeat this analysis for the quantity $\log(W_d)$. We have the expansion

$$\log W_d = \log A(z) - \mathcal{F}(\mathcal{D};\mu)\,\frac{z\,A'(z)}{A(z)}\,\epsilon^{1/2} + \cdots \tag{4.14}$$

or the equivalent expansion

$$(\log W_d)|_{z^p} = 2^p \frac{(2p-1)!}{(p!)^2} \left\{ 1 - p\,\mathcal{F}(D;\mu)\,\epsilon^{1/2} + \cdots \right\}. \tag{4.15}$$

From the above singularity analysis, we may deduce the bulk–boundary distance statistics when $z < 1/8$ in the ensemble of quadrangulations (with a boundary) with a fixed area n, in the limit where $n \to \infty$. Indeed, we may extract the contribution to W_d or $\log W_d$ of these quadrangulations by a contour integral around 0 in the variable g. At large n, this translates into an integral over a real variable ξ upon setting (see [12] for a more detailed discussion)

$$g = \frac{1}{12}\left(1 + \frac{\xi^2}{n}\right). \tag{4.16}$$

We may indeed write at large n

$$\oint \frac{\mathrm{d}g}{2\mathrm{i}\pi} \frac{1}{g^{n+1}}\{\cdot\} \sim \frac{12^n}{\pi n} \int_{-\infty}^{\infty} \mathrm{d}\xi\, \frac{\xi}{\mathrm{i}}\, \mathrm{e}^{-\xi^2}\{\cdot\} \left(1 + \mathcal{O}\left(\frac{\xi^2}{n}\right)\right). \tag{4.17}$$

Setting

$$d = D\,n^{1/4} \tag{4.18}$$

with D finite, we may use the expansion (4.10) with $\epsilon = 1/n$ and $\mu = -\xi^2$ and deduce that at large n

$$W_d|_{g^n} \sim \frac{12^n}{\pi n^{3/2}} z A'(z) \int_{-\infty}^{\infty} \mathrm{d}\xi\, \mathrm{i}\xi\ \mathrm{e}^{-\xi^2} \mathcal{F}(D;-\xi^2) \tag{4.19}$$

since the first (regular) term $A(z)$ in the expansion (4.10) leads to a vanishing integral in ξ by parity. In particular, for $D \to \infty$, we have $\mathcal{F}(D,-\xi^2) \to -\mathrm{i}\xi$ and we obtain

$$W|_{g^n} \sim \frac{12^n}{2\sqrt{\pi} n^{3/2}} z A'(z), \tag{4.20}$$

which may alternatively be obtained directly from the general expression (3.30).

Similarly, we obtain from (4.15) that

$$\begin{aligned}\log W_d|_{g^n} &\sim \frac{12^n}{\pi n^{3/2}}\frac{zA'(z)}{A(z)}\int_{-\infty}^{\infty} \mathrm{d}\xi\, \mathrm{i}\xi\ \mathrm{e}^{-\xi^2}\mathcal{F}(D;-\xi^2)\\ \log W|_{g^n} &\sim \frac{12^n}{2\sqrt{\pi}n^{3/2}}\frac{zA'(z)}{A(z)}.\end{aligned} \tag{4.21}$$

The ratio of these quantities tends at large n to a finite quantity

$$\Phi(D) = \frac{2}{\sqrt{\pi}}\int_{-\infty}^{\infty} \mathrm{d}\xi\, \mathrm{i}\xi\, \mathrm{e}^{-\xi^2}\mathcal{F}(D;-\xi^2) \tag{4.22}$$

which is the *(cumulative) distribution function* for D giving, in the ensemble of pointed quadrangulations with a boundary, the probability that the distance to the boundary of the marked vertex be less than D. In the regime $z < 1/8$, this distribution function is independent of z and identical to the two-point function of the Brownian map [6, 7, 12]. This follows from the fact that, in the regime $z < 1/8$, the length of the boundary does not scale with n but remains finite at large n. This property can be measured as follows: as we have already noticed, the generating function W_0 counts quadrangulations with one marked edge along the boundary. To remove this marking, we must consider instead the generating function $\int_0^z \mathrm{d}z'(W_0(z')-1)/(2z')$, so that the average half-perimeter reads

$$\langle p\rangle_n(z) = \frac{(W_0(z)-1)|_{g^n}}{\int_0^z \mathrm{d}z' \frac{W_0(z')-1}{z'}|_{g^n}}. \tag{4.23}$$

From (3.28), we immediately get that, at large n,

$$(W_0(z)-1)|_{g^n} \sim \frac{12^n}{2\sqrt{\pi}n^{3/2}} z(z\,A(z))'' \tag{4.24}$$

so that $\langle p\rangle_n(z)$ tends to the finite value

$$\langle p\rangle_n(z) \to \frac{z(z\,A(z))''}{(z\,A(z))'-1} = \frac{4z}{(1-8z)(1-\sqrt{1-8z})} \qquad (z<1/8). \tag{4.25}$$

Let us now consider the boundary–boundary distance statistics for $z < 1/8$. When $g \to 1/12$, a sensible scaling limit is now obtained by *keeping d finite* in T_d. This is consistent with the fact that the perimeter itself remains finite and $d \leqslant p$ obviously. For finite d, we now have the expansion

$$f_{d+1} = \frac{d+1}{d+3} - \frac{(d+1)(d+2)}{d+3}\sqrt{\mu}\,\epsilon^{1/2} + \mathcal{O}(\epsilon) \tag{4.26}$$

while the expansion (4.8) still holds. Using (3.32), we obtain

$$T_d = \frac{A(z)^2(2(d+2)-(d+1)A(z))^2}{3(d+1)(d+3)}\,(A(z)-1)^d\,(1+\mathcal{O}(\epsilon)). \tag{4.27}$$

In particular, T_d decays exponentially with d as $\exp(-d/\xi(z))$ with a correlation length

$$\xi(z) = -\frac{1}{\log(A(z)-1)}. \tag{4.28}$$

If we now wish to compute the large n behavior of the term $T_d|_{g^n}$, we have to extract the singular part of T_d, which requires continuing the expansion (4.27) up to order $\epsilon^{3/2}$. This yields a rather complicated and non-universal expression which exhibits the same exponential decay in the distance d.

To conclude, the regime $z < 1/8$ is characterized by a perimeter which remains finite at large n and by boundary–boundary distances which also remain finite and are governed by a non-universal probability law with an exponential decay. This is to be contrasted with the bulk–boundary distances, which scale as $n^{1/4}$ and are governed by the universal two-point function of the Brownian map.

4.3. Scaling limit: the $z > 1/8$ regime

Let us now discuss the situation $z > 1/8$, and more precisely $1/8 < z < 1/4$. In this regime, we have a dominant singularity of the generating functions at $g^{(2)}_{\rm crit}(z)$ and we set

$$g = g^{(2)}_{\rm crit}(z)(1 - \nu\,\epsilon) \tag{4.29}$$

with $\epsilon \to 0$. We then have the expansions

$$W = 2\left(1 - \sqrt{\frac{1-4z}{8z-1}}\sqrt{\nu}\,\epsilon^{1/2} + \cdots\right)$$

$$x = x_{\rm crit}(z) + \mathcal{O}(\epsilon) \quad \text{with} \quad x_{\rm crit}(z) = \frac{16z - 1 - \sqrt{3((8z)^2-1)}}{2(1-4z)}. \tag{4.30}$$

Here $x_{\rm crit}(z)$ is the value of x, as given by (3.4), for $g = g^{(2)}_{\rm crit}(z)$. *Keeping d finite*, the generating function W_d has the expansion

$$W_d = 2\frac{\left(1-x_{\rm crit}^{d+2}\right)\left(1+x_{\rm crit}^{d+2}\right)}{\left(1-x_{\rm crit}^{d+3}\right)\left(1+x_{\rm crit}^{d+1}\right)} - 2\sqrt{\frac{1-4z}{8z-1}}\frac{\left(1-x_{\rm crit}^{d+1}\right)\left(1-x_{\rm crit}^{d+2}\right)^2}{\left(1-x_{\rm crit}^{d+3}\right)\left(1+x_{\rm crit}^{d+1}\right)^2}\sqrt{\nu}\,\epsilon^{1/2} + \cdots \tag{4.31}$$

with $x_{\rm crit} = x_{\rm crit}(z)$ as above. We therefore find in this case a simple square root singularity in $\left(g^{(2)}_{\rm crit} - g\right)$. This singularity (i.e. the term proportional to $\sqrt{\nu}\,\epsilon^{1/2}$ in (4.31)) may be obtained alternatively from the behavior of $W_d|_{z^p}$ at large p. Indeed, from (3.25), we have at large p

$$\begin{aligned} W_d|_{z^p} &\sim \frac{(4\,R)^p}{\sqrt{\pi}\,p^{3/2}}\left\{1-(f_{d+1}-f_d)\sum_{k\geqslant 1}(2k+1)(f_d)^{k-1}\right\} \\ &= \frac{(4\,R)^p}{\sqrt{\pi}\,p^{3/2}}\frac{(1-x^{d+1})(1-x^{d+2})^2}{(1-x^{d+3})(1+x^{d+1})^2}. \end{aligned} \tag{4.32}$$

Upon summing over p with a weight z^p, the p-dependent prefactor gives rise when $4\,R\,z \to 1$ (which happens precisely when g approaches $g^{(2)}_{\rm crit}(z)$ as in (4.29)) to a square root singularity $-2\sqrt{1-4\,R\,z} \sim -2\sqrt{(1-4z)/(8z-1)}\sqrt{\nu}\,\epsilon^{1/2}$, while x simply tends to its value $x_{\rm crit}(z)$ at $g = g^{(2)}_{\rm crit}(z)$. We therefore recover the singular behavior in (4.31) from the contribution of large values of p.

As in the previous section, we can consider quadrangulations with a fixed and large number n of inner faces. This is done again by performing a contour integral in g and setting

$$g = g^{(2)}_{\rm crit}(z)\left(1 + \frac{\zeta^2}{n}\right). \tag{4.33}$$

We may indeed write at large n

$$\oint \frac{{\rm d}g}{2{\rm i}\pi}\frac{1}{g^{n+1}}\{\cdot\} \sim \frac{\left(g^{(2)}_{\rm crit}(z)\right)^{-n}}{\pi n}\int_{-\infty}^{\infty}{\rm d}\zeta\ \frac{\zeta}{\rm i}\ {\rm e}^{-\zeta^2}\{\cdot\}\left(1+\mathcal{O}\left(\frac{\zeta^2}{n}\right)\right). \tag{4.34}$$

Using (4.31) with $\epsilon = 1/n$ and $\nu = -\zeta^2$, we obtain that

$$W_d|_{g^n} \sim \frac{\left(g^{(2)}_{\rm crit}(z)\right)^{-n}}{\sqrt{\pi}n^{3/2}}\sqrt{\frac{1-4z}{8z-1}}\frac{\left(1-x_{\rm crit}^{d+1}\right)\left(1-x_{\rm crit}^{d+2}\right)^2}{\left(1-x_{\rm crit}^{d+3}\right)\left(1+x_{\rm crit}^{d+1}\right)^2}, \qquad W|_{g^n} \sim \frac{\left(g^{(2)}_{\rm crit}(z)\right)^{-n}}{\sqrt{\pi}n^{3/2}}\sqrt{\frac{1-4z}{8z-1}}. \tag{4.35}$$

As for $\log W_d$, we have the expansion

$$\log W_d = \log\left(2\frac{\left(1-x_{\rm crit}^{d+2}\right)\left(1+x_{\rm crit}^{d+2}\right)}{\left(1-x_{\rm crit}^{d+3}\right)\left(1+x_{\rm crit}^{d+1}\right)}\right) - \sqrt{\frac{1-4z}{8z-1}}\frac{\left(1-x_{\rm crit}^{d+1}\right)\left(1-x_{\rm crit}^{d+2}\right)}{\left(1+x_{\rm crit}^{d+1}\right)\left(1+x_{\rm crit}^{d+2}\right)}\sqrt{\nu}\,\epsilon^{1/2} + \cdots \tag{4.36}$$

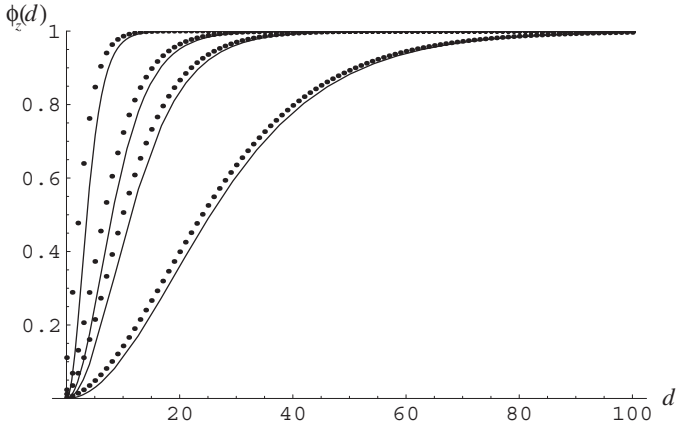

Figure 8. Plots of the (non-universal) cumulative distribution function $\phi_z(d)$ for z approaching the critical value $1/8$ from above, namely $z = 0.13, 0.126, 0.1255$ and 0.1251 (dotted plots from left to right). Beside each plot, we display the corresponding (universal) limiting scaling form (solid line) of equation (4.40).

with a singular part which can be alternatively read off the large p behavior

$$(\log W_d)|_{z^p} \sim \frac{(4\,R)^p}{2\sqrt{\pi}\;p^{3/2}}\left\{1-2\sum_{k\geqslant 1}((f_{d+1})^k-(f_d)^k)\right\}$$
$$= \frac{(4\,R)^p}{2\sqrt{\pi}\;p^{3/2}}\frac{(1-x^{d+1})(1-x^{d+2})}{(1+x^{d+1})(1+x^{d+2})}. \tag{4.37}$$

We immediately deduce the leading behavior

$$\log W_d|_{g^n} \sim \frac{\left(g^{(2)}_{\rm crit}(z)\right)^{-n}}{2\sqrt{\pi}n^{3/2}}\sqrt{\frac{1-4z}{8z-1}}\frac{\left(1-x_{\rm crit}^{d+1}\right)\left(1-x_{\rm crit}^{d+2}\right)}{\left(1+x_{\rm crit}^{d+1}\right)\left(1+x_{\rm crit}^{d+2}\right)}$$
$$\log W|_{g^n} \sim \frac{\left(g^{(2)}_{\rm crit}(z)\right)^{-n}}{2\sqrt{\pi}n^{3/2}}\sqrt{\frac{1-4z}{8z-1}}. \tag{4.38}$$

Taking the ratio $\log W_d|_{g^n}/\log W_d|_{g^n}$, we deduce the large n asymptotic expression $\phi_z(d)$ for the probability that the distance to the boundary of the marked vertex be smaller than or equal to d in the ensemble of pointed quadrangulations with a boundary, namely

$$\phi_z(d) = \frac{(1-(x_{\rm crit}(z))^{d+1})(1-(x_{\rm crit}(z))^{d+2})}{(1+(x_{\rm crit}(z))^{d+1})(1+(x_{\rm crit}(z))^{d+2})}, \tag{4.39}$$

with d finite and $x_{\rm crit}(z)$ as in (4.30). This function is expected to be non-universal. However, when z approaches the critical value $1/8$, we have

$$\phi(d) \sim \tanh^2(d\,\beta(z)) \qquad \text{with} \quad \beta(z) = 2\sqrt{3}\sqrt{z-\tfrac{1}{8}}, \tag{4.40}$$

and we expect that, except for the precise value of β, the above scaling form is universal. The function $\phi_z(d)$ is plotted against its scaling form (4.40) for $z = 0.13, 0.126, 0.1255$ and 0.1251 in figure 8.

From the exponential growth with n of $W_0|_{g^n}$, and from the general formula (4.23), we now have at large n

$$\langle p\rangle_n(z) \sim n \times g^{(2)}_{\rm crit}(z)\frac{\rm d}{{\rm d}z}\big(g^{(2)}_{\rm crit}(z)\big)^{-1} = n \times \frac{8z-1}{1-4z} \quad (1/8 < z < 1/4). \tag{4.41}$$

More precisely, the probability of having a prescribed value of p is proportional to $W_0|_{g^n z^p} z^p/(2p)$. Using the explicit form (3.28) and expanding it at large n with $p \propto n$, we find that, asymptotically, this probability tends to a Gaussian distribution peaked at $p = \langle p\rangle_n(z)$ as above, and with width $\sqrt{n}\,(1-4z)/\sqrt{4z}$.

Let us now consider the boundary–boundary distance statistics in the regime $z > 1/8$. From the expression (3.32) and the expansion (4.30), we see that a sensible scaling limit is now obtained by taking d large as

$$d = D\epsilon^{-1/2} \tag{4.42}$$

with D finite. Using $f_1 = gR^2 \sim (1-4z)/(12z)$ at leading order in ϵ and $f_{d+1} \to x_{\rm crit}(z)$ for large d, we obtain that, in the scaling limit (4.42),

$$T_d \sim \left(8 - \frac{1}{z}\right) {\rm e}^{-2\sqrt{\frac{1-4z}{8z-1}}\sqrt{v}\,D}. \tag{4.43}$$

We can again consider the fixed n ensemble by performing a contour integral in g. Taking $d = Dn^{1/2}$, we now get

$$T_d|_{g^n} \sim \frac{\big(g^{(2)}_{\rm crit}(z)\big)^{-n}}{\pi n}\left(8-\frac{1}{z}\right)\int_{-\infty}^{\infty} d\zeta\,\frac{\zeta}{\rm i}\,{\rm e}^{-\zeta^2+2{\rm i}\,\zeta\sqrt{\frac{1-4z}{8z-1}}\,D} = \frac{\big(g^{(2)}_{\rm crit}(z)\big)^{-n}}{\sqrt{\pi}n}\left(8-\frac{1}{z}\right)\times\sqrt{\frac{1-4z}{8z-1}}\,D\,{\rm e}^{-\frac{1-4z}{8z-1}\,D^2}. \tag{4.44}$$

To have a proper probability density, we must multiply this quantity by the infinitesimal step $n^{1/2}dD$ and normalize it by the generating function of quadrangulations with two marked edges on the boundary, given at large n by

$$2z\frac{\rm d}{{\rm d}z}W_0|_{g^n} \sim 2z\frac{\rm d}{{\rm d}z}\left\{\frac{\big(g^{(2)}_{\rm crit}(z)\big)^{-n}}{\sqrt{\pi}n^{3/2}}\sqrt{\frac{1-4z}{8z-1}}\left(1-\frac{1}{2z}\right)\right\} \sim \frac{\big(g^{(2)}_{\rm crit}(z)\big)^{-n}}{\sqrt{\pi}n^{1/2}}\sqrt{\frac{8z-1}{1-4z}}\left(4-\frac{1}{2z}\right). \tag{4.45}$$

We obtain finally the probability density

$$\rho_{\rm bound.}(D) = 2D\,\frac{1-4z}{8z-1}\,{\rm e}^{-D^2\frac{1-4z}{8z-1}}. \tag{4.46}$$

Here $\rho_{\rm bound.}(D)dD$ measures the probability that the two marked edges on the boundary be at a distance in the quadrangulation in the range $[D, d+dD]$, in the ensemble of quadrangulations with two marked edges on the boundary. It is natural to measure the boundary–boundary distance d in units of the square root of the average half-perimeter $\langle p\rangle_n(z)$, as given by (4.41). This is done by introducing the variable

$$\delta \equiv \frac{d}{\sqrt{n\,\frac{8z-1}{1-4z}}} = D\sqrt{\frac{1-4z}{8z-1}}, \tag{4.47}$$

which remains a finite quantity in the scaling limit. The probability density for the variable δ follows simply from (4.46) and reads

$$\tilde{\rho}_{\text{bound.}}(\delta) = \sqrt{\frac{8z-1}{1-4z}}\,\rho_{\text{bound.}}\left(\delta\sqrt{\frac{8z-1}{1-4z}}\right) = 2\delta\,\mathrm{e}^{-\delta^2}. \tag{4.48}$$

This probability density is independent of z and, as announced in section 2, is identical to the two-point function of the Brownian continuum random tree [25], i.e. a simple Rayleigh law.

To conclude, the regime $z > 1/8$ is characterized by a perimeter which is proportional to n at large n and governed by a Gaussian law peaked at its average value (4.41). The distance of a point in the bulk to this boundary remains finite and is governed by the non-universal distribution $\phi_z(d)$ above. The boundary–boundary distance is of order $n^{1/2}$ and, when measured in natural units given by the square root of the average perimeter, is characterized by the universal two-point function of the Brownian continuum random tree.

4.4. Scaling limit: the critical regime

Let us finally discuss the vicinity of the transition point $z = z_{\text{crit}} = 1/8$. A sensible scaling limit is now obtained by setting

$$\begin{aligned} g &= \tfrac{1}{12}(1-\mu\,\epsilon) \\ z &= \tfrac{1}{8}(1-\mu_B\,\epsilon^{1/2}) \\ d &= D\,\epsilon^{-1/4}, \end{aligned} \tag{4.49}$$

where d may now stand for both the bulk–boundary distance (as in W_d) and the boundary–boundary distance (as in T_d). Using the expansions (4.6) and the expansion

$$W = 2(1-\sqrt{\mu_B+\sqrt{\mu}}\,\epsilon^{1/4}+\cdots), \tag{4.50}$$

we get

$$W_d = 2(1-\mathcal{H}(D;\mu,\mu_B)\,\epsilon^{1/4}+\cdots), \tag{4.51}$$

where

$$\mathcal{H}(D;\mu,\mu_B) = f(D;\mu) + \frac{\mu_B-\sqrt{\mu}/2}{\sqrt{\mu_B+\sqrt{\mu}}+f(D;\mu)} \tag{4.52}$$

with $f(D;\mu)$ given by (4.7). The scaling function $\mathcal{H}(D;\mu,\mu_B)$, obtained here by a direct scaling limit of the discrete expression (3.12) for W_d, can be obtained alternatively as the solution of a nonlinear differential equation as follows: using the expansion for R_d (as obtained for instance via (4.13) for $p=1$ since $R_d = W_d|_{z^1}$)

$$R_d = 2\left(1-\mathcal{F}(D;\mu)\,\epsilon^{1/2}+\cdots\right) \tag{4.53}$$

with $\mathcal{F}(D;\mu)$ given by (4.11), and expanding the recursion relation (3.6) at order $\epsilon^{1/2}$ with W_d as in (4.51), we get the equation

$$\partial_D\mathcal{H}(D;\mu,\mu_B) - \mathcal{H}^2(D;\mu,\mu_B) + \mathcal{F}(D;\mu) + \mu_B = 0. \tag{4.54}$$

The expression (4.52) for $\mathcal{H}(D;\mu,\mu_B)$ is then the unique solution of this equation satisfying $\mathcal{H}(\infty;\mu,\mu_B) = \sqrt{\mu_B+\sqrt{\mu}}$, as required by (4.50). We may also relate our expression to the result of [6] and [7] by introducing the quantity

$$\mathcal{G}^*(D;\mu,\mu_B) \equiv \partial_D\partial_{\mu_B}\mathcal{H}(D;\mu,\mu_B). \tag{4.55}$$

This is indeed the continuous counterpart of the generating function considered in [6] and [7] (in the slightly different context of triangulations) corresponding in our language to pointed

rooted maps with a boundary where the origin-boundary distance has a fixed value $D\epsilon^{-1/4}$ (hence the operator ∂_D) and where the root edge lies anywhere on the boundary (hence the operator ∂_{μ_B}). With our explicit expression for $\mathcal{H}$, it is easy to check that $\mathcal{G}^*$ satisfies

$$\partial_D \mathcal{G}^* = -2\partial_{\mu_B}\left(\mathcal{K}\mathcal{G}^*\right) \qquad \text{with} \quad \mathcal{K} = \mathcal{K}(\mu,\mu_B) \equiv \left(\mu_B - \frac{\sqrt{\mu}}{2}\right)\sqrt{\mu_B+\sqrt{\mu}}. \tag{4.56}$$

This is precisely the equation used in [6] and [7] to determine $\mathcal{G}^*$ and the two-point function.

We have finally the expansion

$$\log W_d = \log(2) - \mathcal{H}(D;\mu,\mu_B)\,\epsilon^{1/4} + \cdots. \tag{4.57}$$

The regime (4.49) corresponds to typical values of the perimeter of order $\epsilon^{-1/2}$. Rather than fixing μ_B, we may alternatively work directly with a fixed value of the half-perimeter p being of order $\epsilon^{-1/2}$, i.e. consider our fixed length generating functions of section 3.3 and set

$$\begin{aligned} g &= \tfrac{1}{12}(1-\mu\epsilon) \\ p &= P\,\epsilon^{-1/2} \\ d &= D\,\epsilon^{-1/4}. \end{aligned} \tag{4.58}$$

Upon setting $k = K\,\epsilon^{-1/4}$, the expression (3.25) translates into

$$\frac{W_d|_{z^p}}{8^p} \sim \epsilon^{3/4}\bar{\mathcal{H}}(D,P;\mu) \quad \text{with}$$

$$\bar{\mathcal{H}}(D,P;\mu) = \frac{\mathrm{e}^{-\sqrt{\mu}P}}{\sqrt{\pi}\,P^{3/2}}\left\{1 + (3\sqrt{\mu} - 2f^2(D;\mu))\int_0^\infty \mathrm{d}K\,\mathrm{e}^{-\frac{K^2}{P}-2f(D;\mu)K}2K\right\}. \tag{4.59}$$

The scaling functions $\mathcal{H}$ and $\bar{\mathcal{H}}$ are then simply related by

$$\mathcal{H}(D;\mu,\mu_B) = \sqrt{\mu_B+\sqrt{\mu}} + \frac{1}{2}\int_0^\infty \mathrm{d}P\,\mathrm{e}^{-\mu_B P}\left(\frac{\mathrm{e}^{-\sqrt{\mu}P}}{\sqrt{\pi}\,P^{3/2}} - \bar{\mathcal{H}}(D,P;\mu)\right). \tag{4.60}$$

For small P, we have in particular

$$\begin{aligned} \bar{\mathcal{H}}(D,P;\mu) &\overset{P\to 0}{\sim} \frac{1}{\sqrt{\pi}\,P^{3/2}}(1-\sqrt{\mu}\,P+\cdots)(1+P(3\sqrt{\mu}-2f^2(D;\mu))+\cdots) \\ &\sim \frac{1}{\sqrt{\pi}\,P^{3/2}}(1-P\mathcal{F}(D;\mu)+\cdots). \end{aligned} \tag{4.61}$$

Note that, as could be expected, this small P behavior matches precisely the large p behavior of $W_d|_{z^p}$ obtained in the regime $z < 1/8$ for finite p, as given by (4.13). For large P, we get instead

$$\begin{aligned} \bar{\mathcal{H}}(D,P;\mu) &\overset{P\to\infty}{\sim} \frac{\mathrm{e}^{-\sqrt{\mu}\,P}}{\sqrt{\pi}\,P^{3/2}}\left(1+\frac{3\sqrt{\mu}-2f^2(D;\mu)}{2f^2(D;\mu)}\right) \\ &= \frac{\mathrm{e}^{-\sqrt{\mu}\,P}}{\sqrt{\pi}\,P^{3/2}}\tanh^2\left(\sqrt{\frac{3}{2}}\,\mu^{1/4}\,D\right). \end{aligned} \tag{4.62}$$

Again, as expected, this expression matches precisely that obtained for $W_d|_{z^p}$ in the regime $z > 1/8$, as given by (4.32), upon considering the scaling limit $p = P\epsilon^{-1/2}$, $R = 2(1-\sqrt{\mu}\epsilon^{1/2})$, $d = D\epsilon^{-1/4}$ and $x = 1-\sqrt{6}\mu^{1/4}\epsilon^{1/4}$. As for $\log W_d$, since, up to a factor of $1/2$, it has the same singularity as W_d, we have

$$\frac{\log W_d|_{z^p}}{8^p} \sim \epsilon^{3/4}\tfrac{1}{2}\bar{\mathcal{H}}(D,P;\mu). \tag{4.63}$$

This behavior can alternatively be obtained by taking directly the scaling limit of (3.26).

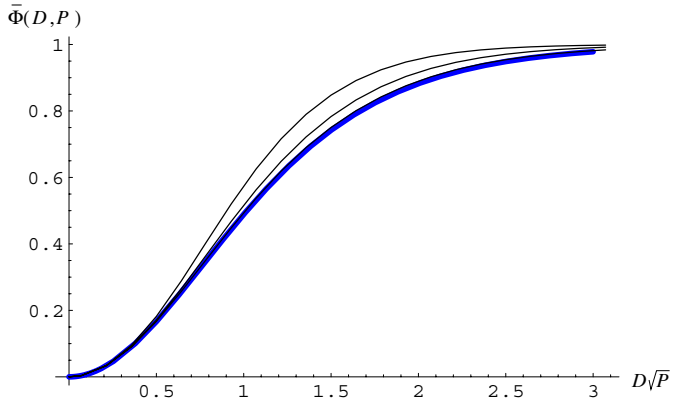

Figure 9. Plots of the cumulative distribution function $\bar{\Phi}(D, P)$ as a function of the scaling variable $D\sqrt{P}$ in the regime of large values of P (thin solid lines) and their comparison with the limiting scaling form of equation (4.67) (thick blue line). The plots represented here are for $P = 1.$, 2. and 5., from left to right.

We can now turn to the fixed n ensemble, with n large and in the critical scaling regime

$$p = P\, n^{1/2} \tag{4.64}$$

with P finite. We then get a cumulative distribution function

$$\bar{\Phi}(D, P) = 2\sqrt{P}\, \mathrm{e}^{P^2/4} \int_{-\infty}^{\infty} \mathrm{d}\xi\, \frac{\xi}{\mathrm{i}}\, \mathrm{e}^{-\xi^2}\, \bar{\mathcal{H}}(D, P; -\xi^2), \tag{4.65}$$

which measures the probability that a vertex chosen uniformly at random in the quadrangulation be at a rescaled distance less than D from the boundary. This distribution function is plotted in figure 2 for $P = 0.01$, 0.1, 0.5, 1.0, 2.0 and 5.0. For fixed P and small D, we have the expansion

$$\bar{\Phi}(D, P) = \tfrac{3}{4} P\, D^2 - \tfrac{3}{8}(P^2 - 1) D^4 + \cdots. \tag{4.66}$$

For fixed D and small P, using (4.61), we immediately see that $\bar{\Phi}(D, P) \to \Phi(D)$ as expected. This property is illustrated in figure 2. Note that the small D and small P limits do not commute.

On the other hand, when P is large, using (4.62) and evaluating the integral over ξ by a saddle point estimate, we deduce that

$$\bar{\Phi}(D, P) \overset{P\to\infty}{\to} \tanh^2\left(\tfrac{\sqrt{3}}{2} D\, \sqrt{P}\right). \tag{4.67}$$

This property is illustrated in figure 9 for $P = 1.$, 2. and 5.

Concerning the boundary–boundary distance, using the expression (3.33), we get in the scaling regime (4.58) the limiting expression for $T_d|_{z^p}$:

$$\frac{T_d|_{z^p}}{8^p} \sim \frac{8}{3}\epsilon \frac{\mathrm{e}^{-\sqrt{\mu}\, P - \frac{D^2}{P}}}{\sqrt{\pi}\, P^{7/2}} \{(2D^3 - 3D\, P) + (4D^2 P - 2P^2) f(D; \mu) + 2DP^2 f^2(D; \mu)\}. \tag{4.68}$$

It is natural to measure the boundary–boundary distances in units of $\sqrt{p}$, i.e. write $d = \delta\sqrt{p}$ or equivalently

$$D = \delta\sqrt{P}. \tag{4.69}$$

In the variable δ, equation (4.70) translates into

$$\frac{T_d|_{z^p}}{8^p} \sim \frac{8}{3}\epsilon \frac{\mathrm{e}^{-\sqrt{\mu}\,P-\delta^2}}{\sqrt{\pi}\,P^2}\{(2\delta^3-3\delta)+(4\delta^2-2)\sqrt{P}\,f(\sqrt{P}\delta;\,\mu)+2\delta(\sqrt{P}\,f(\sqrt{P}\delta;\,\mu))^2\}. \quad (4.70)$$

At small P, we have the expansion

$$\frac{T_d|_{z^p}}{8^p} \overset{P\to 0}{\sim} \frac{8}{3}\epsilon \frac{\mathrm{e}^{-\delta^2}}{\sqrt{\pi}\,P^2}\left\{(\delta+2\delta^3)-\frac{5\delta+6\delta^3+2\delta^5}{10}\mu P^2+\frac{35\delta+28\delta^3+12\delta^5+3\delta^7}{105}\mu^{3/2}P^3+\cdots\right\} \quad (4.71)$$

while at large P, we have

$$\frac{T_d|_{z^p}}{8^p} \overset{P\to\infty}{\sim} 4\sqrt{\mu}\,\epsilon\,\frac{\mathrm{e}^{-\sqrt{\mu}\,P}}{\sqrt{\pi}\,P}\{2\delta\,\mathrm{e}^{-\delta^2}+\cdots\}. \quad (4.72)$$

We turn finally to fixed values of n and p, in the critical scaling regime $n\to\infty$ with the ratio $P = p/n^{1/2}$ fixed. Using (4.70) with $\epsilon = 1/n$ and $\mu = -\xi^2$, multiplying by the elementary step $n^{1/4}dD$ and normalizing by $2pW_0|_{g^n z^p}$, which behaves as

$$\frac{2pW_0|_{g^n z^p}}{8^p} \sim \frac{12^n}{\pi n^{7/4}}\,\mathrm{e}^{-P^2/4}\,P^{3/2}, \quad (4.73)$$

we get a critical probability density for the rescaled boundary–boundary distance $D = d\cdot n^{-1/4}$:

$$\bar{\rho}_{\text{bound.}}(D,\,P) = \frac{4}{3P^4}\,\mathrm{e}^{-D^2/P}\{(2D^3-3DP)+(4D^2P-2P^2)\sigma_1(D,\,P)+2DP^2\sigma_2(D,\,P)\}$$

$$\text{with}\qquad \sigma_1(D,\,P) = \frac{2\,\mathrm{e}^{P^2/4}}{\sqrt{\pi}\,P}\int_{-\infty}^{\infty}\mathrm{d}\xi\,\frac{\xi}{\mathrm{i}}\,\mathrm{e}^{-\xi^2+\mathrm{i}\xi P}f(D;\,-\xi^2)$$

$$\sigma_2(D,\,P) = \frac{2\,\mathrm{e}^{P^2/4}}{\sqrt{\pi}\,P}\int_{-\infty}^{\infty}\mathrm{d}\xi\,\frac{\xi}{\mathrm{i}}\,\mathrm{e}^{-\xi^2+\mathrm{i}\xi P}f^2(D;\,-\xi^2). \quad (4.74)$$

As before, it is natural to measure the boundary distances in units of $\sqrt{p}$, i.e. write $d = \delta\sqrt{p}$ or equivalently $D = \delta\sqrt{P}$. We find for δ a probability density

$$\tilde{\rho}_{\text{bound.}}(\delta,\,P) = \frac{4}{3P^2}\,\mathrm{e}^{-\delta^2}\{(2\delta^3-3\delta)+(4\delta^2-2)\tilde{\sigma}_1(\delta,\,P)+2\delta\tilde{\sigma}_2(\delta,\,P)\}$$

$$\text{with}\qquad \tilde{\sigma}_1(\delta,\,P) = \frac{2\,\mathrm{e}^{P^2/4}}{\sqrt{\pi}\sqrt{P}}\int_{-\infty}^{\infty}\mathrm{d}\xi\,\frac{\xi}{\mathrm{i}}\,\mathrm{e}^{-\xi^2+\mathrm{i}\xi P}f(\delta\sqrt{P};\,-\xi^2)$$

$$\tilde{\sigma}_2(\delta,\,P) = \frac{2\,\mathrm{e}^{P^2/4}}{\sqrt{\pi}}\int_{-\infty}^{\infty}\mathrm{d}\xi\,\frac{\xi}{\mathrm{i}}\,\mathrm{e}^{-\xi^2+\mathrm{i}\xi P}f^2(\delta\sqrt{P};\,-\xi^2). \quad (4.75)$$

This probability density is plotted in figure 3 for $P = 0.5$, 1.0, 1.5, 2.0, 3.0, 5.0 and 10.0.

At small P, we find in particular from (4.71) that

$$\tilde{\rho}_{\text{bound.}}(\delta,\,P) \overset{P\to 0}{\to} \frac{2}{105}\mathrm{e}^{-\delta^2}(35\delta+28\delta^3+12\delta^5+3\delta^7). \quad (4.76)$$

At large P, we have the simple result

$$\tilde{\rho}_{\text{bound.}}(\delta,\,P) \overset{P\to\infty}{\to} 2\,\delta\,\mathrm{e}^{-\delta^2}. \quad (4.77)$$

Repeating the above analysis for the refined generating function $T_d(s,s')$ of equation (3.34), we have access to the refined probability $\tilde{\rho}_{\text{bound.}}(\delta,u,P)$ that the vertex of the boundary at rescaled distance $2Pu$ ($0\geqslant u\geqslant 1$) *along the boundary* from a given

vertex (chosen uniformly at random on the boundary) be at rescaled distance $\delta\sqrt{P}$ *in the quadrangulation* from this vertex. This probability density reads

$$\tilde{\rho}_{\text{bound.}}(\delta, u, P) = \frac{1}{6\sqrt{\pi}P^2}\frac{\mathrm{e}^{-\frac{\delta^2}{4u(1-u)}}}{u^{5/2}(1-u)^{5/2}}\{(\delta^2-2u)(\delta^2-2(1-u)) + 2\delta(\delta^2-4u(1-u))\tilde{\sigma}_1(\delta, P)+4\delta^2u(1-u)\tilde{\sigma}_2(\delta, P)\}. \tag{4.78}$$

We have in particular, for small P,

$$\tilde{\rho}_{\text{bound.}}(\delta, u, P) \overset{P\to 0}{\to} \frac{1}{6\sqrt{\pi}}\frac{\mathrm{e}^{-\frac{\delta^2}{4u(1-u)}}}{u^{5/2}(1-u)^{5/2}}\frac{\delta^4}{140}\{70+21\delta^2+3\delta^4-42u(1-u)(\delta^2+5)\} \tag{4.79}$$

while, for large P,

$$\tilde{\rho}_{\text{bound.}}(\delta, u, P) \overset{P\to\infty}{\to} \frac{1}{2\sqrt{\pi}}\frac{\delta^2\,\mathrm{e}^{-\frac{\delta^2}{4u(1-u)}}}{u^{3/2}(1-u)^{3/2}}. \tag{4.80}$$

A simpler characterization of the distance in the quadrangulation of two boundary vertices at distance $2Pu$ along the boundary is through the corresponding average value

$$\langle\delta(u)\rangle_P \equiv \int_0^\infty \mathrm{d}\delta\ \delta\ \tilde{\rho}_{\text{bound.}}(\delta, u, P). \tag{4.81}$$

This average value is plotted in figure 10 for $P = 0.5$, 1.0, 1.5, 2.0, 3.0, 5.0 and 10.0. For P small, we get in particular

$$\langle\delta(u)\rangle_P \overset{P\to 0}{\to} \frac{16}{105}\sqrt{\frac{u(1-u)}{\pi}}\{35+21u(1-u)+36u^2(1-u)^2\} \tag{4.82}$$

while, for P large, we have

$$\langle\delta(u)\rangle_P \overset{P\to\infty}{\to} 4\sqrt{\frac{u(1-u)}{\pi}}. \tag{4.83}$$

To conclude, quadrangulations with a boundary display an interesting scaling behavior when both the number n of inner faces and the length $2p$ of the boundary become large, keeping the ratio $P = p/n^{1/2}$ fixed. In this regime, the bulk–boundary distances scale as $n^{1/4}$ and are characterized by a *universal distribution function* $\bar{\Phi}(D, P)$ which interpolates between the (cumulative) two-point function of $\Phi(D)$ the Brownian map for small P to a simple $\tanh^2$ function in the variable $D\sqrt{P}$ at large P. As for the boundary–boundary distances, they scale as the square root of the perimeter and are characterized by a *universal probability density* $\tilde{\rho}_{\text{bound.}}(\delta, P)$ which interpolates between the two-point function of the Brownian continuum random tree when P is large to the small P expression (4.76). Note that this latter formula, even if it looks rather involved, is expected to be universal, and so are the formulae (4.79) and (4.82).

5. Self-avoiding boundary

5.1. Generating functions

So far, we have considered quadrangulations whose boundary may contain separating vertices or edges, corresponding to vertices or edges encountered several times along the contour. We may instead consider quadrangulations *with a self-avoiding boundary*, i.e. demand that the $2p$ vertices (and consequently the $2p$ edges) along the contour be all distinct. We shall denote by $\tilde{W}_d$ the generating function for quadrangulations with a self-avoiding boundary having a

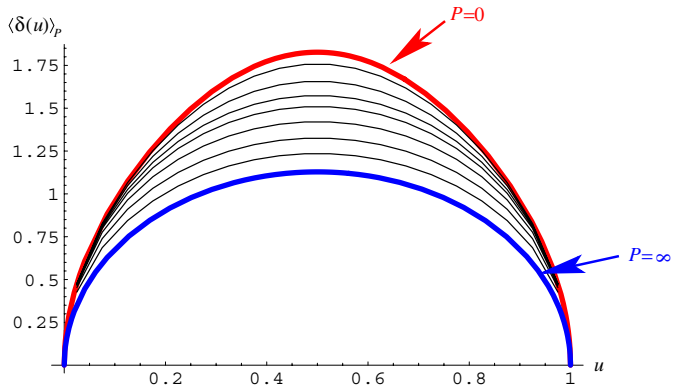

Figure 10. The average value $\langle\delta(u)\rangle$ (measured in units of $\sqrt{P}$) for the distance in the quadrangulation of two boundary points at rescaled distance u (measured in units of $2P$) along the boundary, here for $P = 0.5$, 1.0, 1.5, 2.0, 3.0, 5.0 and 10.0 (thin lines from top to bottom). The plots interpolate between two limiting laws (thick lines): the non-trivial (but universal) law of equation (4.82) for $P \to 0$ and the simple semi-circle law of equation (4.83) for $P \to \infty$.

marked vertex at distance *smaller than or equal to d* from the boundary, and as before with a marked 'closest edge', i.e. a boundary edge incident to a vertex at minimal distance from the marked vertex and oriented counterclockwise around the bulk of the quadrangulation. As before, when $d = 0$, these markings reduce to the choice of a boundary edge oriented clockwise around the bulk. In $\tilde{W}_d$, we weight each configuration by a factor g per inner face and a factor $\sqrt{Z}$ per edge of the boundary. For convenience, we decide to also add to the configurations counted by $\tilde{W}_d$ the empty configuration (weight 1) and the configuration with $p = 1$ and $n = 0$ (weight Z) corresponding to a single edge embedded in the external face, although the boundary is not self-avoiding in this case. In other words, we take the convention that $\tilde{W}_d|_{g^0} = 1 + Z$ in the following. With this convention, it is easy to check that we have the combinatorial identity

$$W_0(g, z) = \tilde{W}_0(g, Z) \qquad \text{with} \quad Z = zW_0^2(g, z). \tag{5.1}$$

Indeed, considering the root edge in any (non-empty) configuration counted by W_0, with the external face on its right, it belongs to some irreducible component which is either a quadrangulation of non-zero area, with a self-avoiding boundary of length, say $2p_0$ with $p_0 \geqslant 1$, or a single edge ($p_0 = 1$) if the root edge is a separating edge (see figure 11 for an illustration). The configurations in the latter case are counted by $zW_0^2(g, z)$, while those in the former case are counted by $(\tilde{W}_0 - 1 - Z)|_{Z^{p_0}} \times \left(zW_0^2(g, z)\right)^{p_0}$ since we may attach to each vertex of the self-avoiding boundary of the irreducible component a configuration counted by $W_0(g, z)$. Summing over p_0, we end up with the relation (5.1).

For $d > 0$, we have the slightly different relation

$$W_d(g, z) - W_0(g, z) = W_0(g, z)\left(\tilde{W}_d(g, Z) - \tilde{W}_0(g, Z)\right) \qquad \text{with} \quad Z = zW_0^2(g, z). \tag{5.2}$$

Indeed, $W_d - W_0$ counts configurations with a marked vertex strictly in the bulk of the quadrangulation, at distance less than or equal to d and with a marked closest edge. The marked vertex belongs to one particular irreducible component and its distance to the whole boundary is equal to its distance to the self-avoiding boundary of this component. The most general configuration is then obtained by attaching to each vertex of the self-avoiding

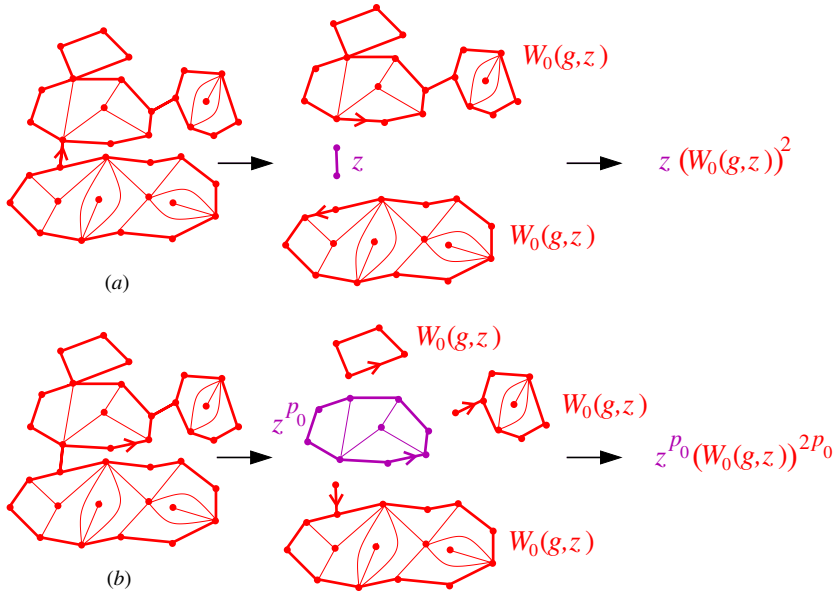

Figure 11. A schematic picture of equation (5.1). In any rooted quadrangulation with a boundary, the root edge selects a particular irreducible component (middle component in magenta) which may be either a single edge (*a*) or an irreducible component with non-zero area and self-avoiding boundary of perimeter $2p_0$. The other irreducible components may be reassembled into (possibly empty) quadrangulations with a generic boundary attached to each of the two endpoints of the edge (case (*a*)) or to each of the $2p_0$ boundary vertices of the selected irreducible component (case (*b*)). These attached quadrangulations are naturally rooted and each of them gives rise to a factor $W_0(g, z)$.

boundary of the irreducible component a configuration counted by $W_0(g, z)$, leading again to the effective weight $Z = zW_0^2$ in the generating function for the irreducible component (see figure 12 for an illustration). Finally, the marked closest edge on the original configuration starts to form a particular closest *vertex* on the self-avoiding boundary which in turn selects a closest edge on the self-avoiding boundary, leading eventually to $\tilde{W}_d - \tilde{W}_0$. The marking of the original closest edge induces a splitting in two parts of the contour of the configuration attached to the marked closest vertex on the self-avoiding boundary, resulting in an extra multiplicative factor $W_0(g, z)$ in (5.2).

It is more natural to consider configurations without a marked closest edge. In the case of a non-self-avoiding boundary, this was done by changing W_d into $\log W_d$. Here, we find that suppressing the marking of the closest edge results in replacing the generating function $\tilde{W}_d$ by a modified generating function

$$\tilde{W}'_d \equiv \tilde{W}_0 - 1 + \log(\tilde{W}_d - (\tilde{W}_0 - 1)). \tag{5.3}$$

The proof of this relation is sketched as follows. It is equivalent to exhibiting a generating function S_d such that

$$\begin{aligned} \tilde{W}_d - (\tilde{W}_0 - 1) &= \sum_{k\geqslant 0} (S_d)^k \\ \tilde{W}'_d - (\tilde{W}_0 - 1) &= \sum_{k\geqslant 1} \frac{1}{k} (S_d)^k. \end{aligned} \tag{5.4}$$

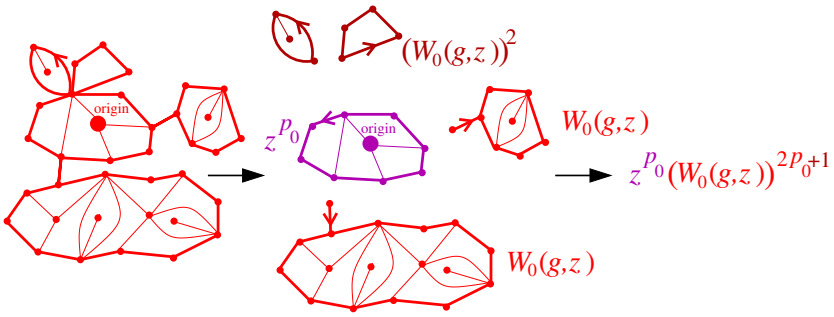

Figure 12. A schematic picture of equation (5.2). In any pointed-rooted quadrangulation with a boundary counted by $W_d - W_0$, the origin vertex lies strictly in the bulk of some particular irreducible component (middle component in magenta), with the self-avoiding boundary of perimeter $2p_0$. The other irreducible components may be reassembled into $2p_0$ naturally rooted quadrangulations with a generic boundary attached to the $2p_0$ boundary vertices of the selected irreducible component. One of these quadrangulations contains the originally marked closest edge, inducing a natural splitting in two parts (upper components in dark red) which results in an extra factor $W_0(g, z)$.

Combinatorially, both left hand sides are generating functions for pointed quadrangulations with a self-avoiding boundary, such that the origin-loop distance is between 1 and d, with an additional marking of a closest boundary vertex in the first case (note that the markings of an edge or of a vertex are equivalent of self-avoiding boundaries). Clearly, we shall look for a decomposition according to the number k of such closest vertices. A possible way is to decompose the map into k 'slices' by cutting along each *leftmost geodesic* from a closest vertex to the origin; see figure 13. Each slice is itself a quadrangulation with a self-avoiding boundary and has three distinguished vertices on the boundary: two of them, say v_1 and v_2, correspond to two clockwise consecutive closest boundary vertices in the original map and the third, say v_3, is the point where their outgoing leftmost geodesics merge (note that v_3 is not necessarily the origin). Furthermore, the slice contour consists of three segments (v_1v_2), (v_2v_3) and (v_3v_1) of non-zero length, and the following properties hold within the slice:

- (v_3v_1) and (v_2v_3) are geodesics of the same length ℓ, hereafter called the depth of the slice, with $1 \leqslant \ell \leqslant d$,
- there is no other geodesic from v_1 to v_3 (due to our convention of cutting along leftmost geodesics),
- all vertices on (v_1v_2) distinct from v_1 and v_2 are at distance strictly larger than ℓ from v_3.

Let S_d be the generating function for slices satisfying the above characterization, with a weight g per face and $\sqrt{Z}$ per edge of (v_1v_2). Then, we have a bijective decomposition of the original map into a linear or cyclic sequence of slices, depending on whether a closest boundary vertex is marked or not. Note that the slices obtained in the decomposition do not necessarily have the same depth, and that the maximal depth is equal to the origin-loop distance. Omitting further details of the proof, the identities (5.4) are established.

The generating function for pointed quadrangulations with a self-avoiding boundary with origin-boundary distance equal to d is

$$\tilde{G}_d = \tilde{W}'_d - \tilde{W}'_{d-1}, \qquad \tilde{G}_0 = \tilde{W}'_0 = \tilde{W}_0 - 1, \tag{5.5}$$

which yields the formula (2.12) announced in section 2.

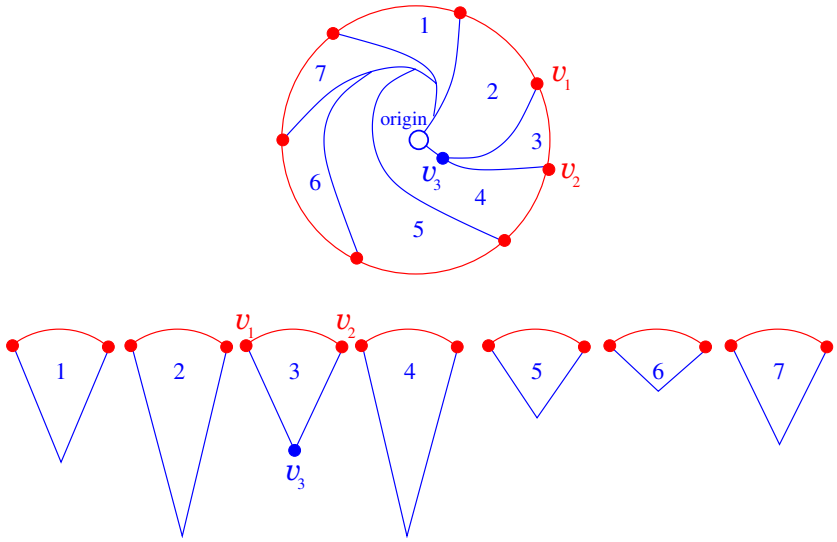

Figure 13. A schematic picture of the decomposition of a pointed quadrangulation with a self-avoiding boundary, whose origin lies strictly in the bulk and with k closest vertices on the boundary (here $k = 7$), into k slices, as defined in the text. From each closest vertex on the boundary (red dots), we draw the leftmost geodesic path to the origin (blue circle). Note that these geodesics cannot cross but may merge before reaching the origin (as in v_3). This splits the quadrangulation into k triangular slices whose depths are generally different, with the maximal depth being equal to the origin-boundary distance.

Let us now derive explicit expressions for $\tilde{W}_d$ and $\tilde{W}'_d$. From (5.1) and from the general expression (3.15) for W_0, we immediately deduce that

$$\tilde{W}_0(g, Z) = \tilde{W}(1 - f_1\,(\tilde{W} - 1)), \tag{5.6}$$

where

$$\tilde{W} \equiv \tilde{W}(g, Z) = W(g, z(g, Z)) \qquad \text{with} \quad z(g, Z) \text{ given implicitly by}$$
$$Z = z(g, Z) W_0^2(g, z(g, Z)) = z(g, Z)\tilde{W}_0^2(g, Z). \tag{5.7}$$

Writing these equations as

$$\tilde{W} = 1 + z(g, Z)\, R\, \tilde{W}^2$$
$$Z = z(g, Z)(\tilde{W}(1 - f_1(\tilde{W} - 1)))^2 \tag{5.8}$$

and eliminating $z(g, Z)$, we deduce the relation

$$Z = \frac{\tilde{W} - 1}{R}(1 - f_1(\tilde{W} - 1))^2 \tag{5.9}$$

which determines $\tilde{W}$ as a function of g and Z. As for $\tilde{W}_d$ for $d > 0$, we deduce from (5.2) and from the general expression (3.12) for W_d that

$$\tilde{W}_d(g, Z) = \frac{1}{1 - f_1(\tilde{W} - 1)} \times \frac{1 - (\tilde{W} - 1) f_{d+1}}{1 - (\tilde{W} - 1) f_d} + \tilde{W}_0 - 1 \tag{5.10}$$

with $\tilde{W}$ related to Z as in (5.9) . Note that the quantity $\tilde{W}_d$ depends on Z only via $\tilde{W}$ but that, unlike generic boundaries, $\tilde{W}$ is not the limit of $\tilde{W}_d$ for $d \to \infty$. Finally, we have

$$\tilde{W}'_d(g, Z) = \log\left(\frac{1}{1 - f_1(\tilde{W} - 1)} \times \frac{1 - (\tilde{W} - 1) f_{d+1}}{1 - (\tilde{W} - 1) f_d}\right) + \tilde{W}_0 - 1. \tag{5.11}$$

As before, $\tilde{W}_d$ and $\tilde{W}'_d$ are Lagrangean generating functions and we may extract an explicit expression for their Z^p term. Writing (5.9) as

$$Z = \frac{\tilde{w}}{R}(1 - f_1\tilde{w})^2 \tag{5.12}$$

upon introducing the quantity

$$\tilde{w} \equiv \tilde{W} - 1, \tag{5.13}$$

we may easily transform any contour integral in the variable Z into a contour integral in the variable $\tilde{w}$, namely

$$\oint \frac{\mathrm{d}Z}{2\mathrm{i}\pi}\frac{1}{Z^{p+1}}\{\cdot\} = R^p \oint \frac{\mathrm{d}\tilde{w}}{2\mathrm{i}\pi}\frac{1}{\tilde{w}^{p+1}}\frac{1-3f_1\tilde{w}}{(1-f_1\tilde{w})^{2p+1}}\{\cdot\}. \tag{5.14}$$

Using (5.6), which we write as

$$\tilde{W}_0 = (1+\tilde{w})(1-f_1\tilde{w}), \tag{5.15}$$

and $f_1 = g\,R^2$, we obtain

$$\tilde{W}_0|_{Z^p} = (gR^3)^p \frac{(3p-3)!}{p!(2p-1)!}\left(\frac{p}{g\,R^2} + 2 - 3p\right) \tag{5.16}$$

for $p \geqslant 1$, and $\tilde{W}_0|_{Z^0} = 1$. Extracting the g^n term of the right-hand side, we deduce the equivalent formula

$$\tilde{W}_0|_{g^n Z^p} = 3^{n-p}\frac{(3p)!}{p!(2p-1)!}\frac{(2n+p-1)!}{(n-p+1)!(n+2p)!}, \tag{5.17}$$

valid for all $n \geqslant 0$, $1 \leqslant p \leqslant n+1$.

As for $\tilde{W}_d$, we get upon expanding (5.10) in $\tilde{w} = \tilde{W} - 1$ the expression

$$\tilde{W}_d = \frac{1}{1-f_1\tilde{w}}\left(1 - \tilde{w}\,(f_{d+1} - f_d)\sum_{k\geqslant 1}(\tilde{w}\,f_d)^{k-1}\right) + \tilde{W}_0 - 1 \tag{5.18}$$

from which we deduce

$$\begin{aligned}\tilde{W}_d|_{Z^p} &= (gR^3)^p\left\{\binom{3p}{p} - 2\binom{3p}{p-1} - (f_{d+1}-f_d)\sum_{k\geqslant 1}\frac{\binom{3p-k}{p-k} - 2\binom{3p-k}{p-1-k}}{(g\,R^2)^k}(f_d)^{k-1}\right\} \\ &\quad + \tilde{W}_0|_{Z^p} - \delta_{p,0} \\ &= (gR^3)^p\left\{\frac{(3p)!}{p!(2p+1)!} - (f_{d+1}-f_d)\sum_{k=1}^{p}\frac{(3p-k)!}{(p-k)!(2p+1)!}\frac{(2k+1)}{(g\,R^2)^k}(f_d)^{k-1}\right\} \\ &\quad + \tilde{W}_0|_{Z^p} - \delta_{p,0}.\end{aligned} \tag{5.19}$$

By a similar argument, we have

$$\begin{aligned}\tilde{W}'_d|_{Z^p} &= (gR^3)^p\left\{\frac{(3p-1)!}{p!(2p)!} - 2\sum_{k=1}^{p}\frac{(3p-k-1)!}{(p-k)!(2p)!}\frac{1}{(g\,R^2)^k}\left((f_{d+1})^k - (f_d)^k\right)\right\} \\ &\quad + \tilde{W}_0|_{Z^p}\end{aligned} \tag{5.20}$$

for $p \geqslant 1$.

5.2. Critical behavior and scaling limits

As before, the generating functions $\tilde{W}_d$ and $\tilde{W}'_d$ have a first singularity at $g = 1/12$, irrespectively of the value of Z. A second singularity comes from $\tilde{W}$ which, from (5.9), is singular when

$$\tfrac{27}{4} g\, R^3\, Z = 1. \tag{5.21}$$

This equality may occur only when $Z \geqslant 2/9$ and it defines a critical line $g = \tilde{g}_{\rm crit}(Z)$, with

$$\tilde{g}_{\rm crit}(Z) = \tfrac{1}{32}((4+9Z)\sqrt{16Z+9Z^2} - 9Z(4+3Z)) \qquad (Z \geqslant 2/9). \tag{5.22}$$

For $Z > 2/9$, we have $\tilde{g}_{\rm crit}(Z) < 1/12$ so that this new value determines the radius of convergence in g of $\tilde{W}_d$. As before, we have a change of determination of the radius of convergence at the critical value

$$Z_{\rm crit} = \tfrac{2}{9}, \tag{5.23}$$

corresponding to a transition between two differently behaved regimes.

To study the regime $Z < 2/9$, we set as before

$$\begin{aligned} g &= \tfrac{1}{12}(1 - \mu\,\epsilon) \\ d &= D\,\epsilon^{-1/4} \end{aligned} \tag{5.24}$$

and we use the expansion (5.19) to get

$$\begin{aligned} \tilde{W}_d|_{Z^p} &= \tilde{W}_0|_{Z^p} - \delta_{p,0} + \left(\frac{2}{3}\right)^p \Big\{ \frac{(3p)!}{p!(2p+1)!}(1 - 3p\,\sqrt{\mu}\,\epsilon^{1/2}) \\ &\quad - (2f^2(D;\mu) - 3\sqrt{\mu})\,\epsilon^{1/2} \sum_{k=1}^{p} 3^k \frac{(3p-k)!}{(p-k)!(2p+1)!}(2k+1) \Big\} + \cdots \\ &= \tilde{W}_0|_{Z^p} - \delta_{p,0} + \left(\frac{2}{3}\right)^p \frac{(3p)!}{p!(2p+1)!} \left\{1 - 3p\,\mathcal{F}(D;\mu)\,\epsilon^{1/2} + \cdots\right\}. \end{aligned} \tag{5.25}$$

Here we have used the identity

$$\sum_{k=1}^{p} 3^k \frac{(3p-k)!}{(p-k)!(2p+1)!}(2k+1) = 3\,\frac{(3p)!}{(p-1)!(2p+1)!} \tag{5.26}$$

obtained by writing the summand on the left-hand side as $\alpha_k - \alpha_{k+1}$ with $\alpha_k \equiv 3^k \binom{3p-k-1}{p-1}$. Similarly, we have

$$\tilde{W}'_d|_{Z^p} = \tilde{W}_0|_{Z^p} + \left(\frac{2}{3}\right)^p \frac{(3p-1)!}{p!(2p)!}\{1 - 3p\,\mathcal{F}(D;\mu)\,\epsilon^{1/2} + \cdots\} \tag{5.27}$$

for $p \geqslant 1$.

Finally, from (5.16), we have

$$\tilde{W}_0|_{Z^p} = 2\left(\frac{2}{3}\right)^p \frac{(3p-3)!}{p!(2p-1)!}(1 + \mathcal{O}(\epsilon)) \tag{5.28}$$

for $p > 0$ and $\tilde{W}_0|_{Z^0} = 1$. Summing (5.25) over p with a weight Z^p, we obtain

$$\begin{aligned} \tilde{W}_d &= \tilde{A}_0(Z) + \tilde{A}(Z) - 3Z\tilde{A}'(Z)\,\mathcal{F}(D;\mu)\,\epsilon^{1/2} + \cdots \\ &\text{with} \quad \tilde{A}_0(Z) = 2\sum_{p\geqslant 1}\left(\frac{2}{3}\right)^p Z^p \frac{(3p-3)!}{p!(2p-1)!} \\ &= \frac{2}{3}\left(-1 + {}_2F_1\left(\left\{-\frac{2}{3}, -\frac{1}{3}\right\}, \left\{\frac{1}{2}\right\}, \frac{9Z}{2}\right)\right) \\ &\tilde{A}(Z) = \sum_{p\geqslant 0}\left(\frac{2}{3}\right)^p Z^p \frac{(3p)!}{p!(2p+1)!} = \sqrt{\frac{2}{Z}}\,\sin\left(\frac{1}{3}\arcsin\left(3\sqrt{\frac{Z}{2}}\right)\right), \end{aligned} \tag{5.29}$$

while

$$\tilde{W}'_d = \tilde{A}_0(Z) + \log \tilde{A}(Z) - \frac{3Z\tilde{A}'(Z)}{\tilde{A}(Z)}\,\mathcal{F}(D;\mu)\,\epsilon^{1/2} + \cdots. \tag{5.30}$$

Going to a fixed n ensemble, we deduce from this expansion that

$$\begin{aligned} \tilde{W}'_d|_{g^n} &\sim \frac{12^n}{\pi n^{3/2}}\frac{3Z\tilde{A}'(Z)}{\tilde{A}(Z)}\int_{-\infty}^{\infty} \mathrm{d}\xi\ \mathrm{i}\xi\ \ \mathrm{e}^{-\xi^2}\mathcal{F}(D;-\xi^2) \\ \tilde{W}'_\infty|_{g^n} &\sim \frac{12^n}{2\sqrt{\pi}n^{3/2}}\frac{3Z\tilde{A}'(Z)}{\tilde{A}(Z)} \qquad \text{where} \quad \tilde{W}'_\infty \equiv \lim_{d\to\infty}\tilde{W}'_d \end{aligned} \tag{5.31}$$

at large n so that, taking the ratio of these quantities, we get *the same asymptotic distribution function* $\Phi(D)$ as in section 3 for the rescaled distance D. In the $Z < 2/9$ regime, the length of the boundary does not scale with n and quadrangulations with a self-avoiding boundary stay, in the scaling limit, in the universality class of the Brownian map.

To study the regime $Z > 2/9$, we must now set

$$Z = \tilde{g}_{\mathrm{crit}}(Z)(1 - \tilde{\nu}\,\epsilon) \tag{5.32}$$

and keep d finite. We introduce the notations

$$\begin{aligned} \tilde{x}_{\mathrm{crit}}(Z) &\equiv \frac{1}{16}(27Z - 8 + 9\sqrt{Z(16+9Z)} \\ &\quad - \sqrt{6}\sqrt{243Z^2 + 144Z - 32 + 3(27Z-8)\sqrt{Z(16+9Z)}}) \\ \tilde{f}_d^{\mathrm{crit}} &\equiv \tilde{x}_{\mathrm{crit}}(Z)\frac{1-(\tilde{x}_{\mathrm{crit}}(Z))^d}{1-(\tilde{x}_{\mathrm{crit}}(Z))^{d+2}}. \end{aligned} \tag{5.33}$$

Here $\tilde{x}_{\mathrm{crit}}(Z)$ is simply the value of x when $g = \tilde{g}_{\mathrm{crit}}(Z)$. With these notations, we have the expansion

$$\tilde{W} = \left(1 + \frac{3}{\tilde{f}_1^{\mathrm{crit}}}\right) - \tilde{C}(Z)\sqrt{\tilde{\nu}}\,\epsilon^{1/2}, \tag{5.34}$$

where $\tilde{C}(Z)$ is some function of Z (with no singularity for $Z > 2/9$) which we do not make explicit. We then find the expansion

$$\begin{aligned} \tilde{W}_d &= \left\{\frac{4+21\tilde{f}_1^{\mathrm{crit}}}{18\tilde{f}_1^{\mathrm{crit}}} + \frac{3}{2}\frac{(\tilde{f}_d^{\mathrm{crit}} - \tilde{f}_{d+1}^{\mathrm{crit}})}{(3\tilde{f}_1^{\mathrm{crit}} - \tilde{f}_d^{\mathrm{crit}})}\right\} \\ &\quad - \tilde{C}(Z)\sqrt{\tilde{\nu}}\,\epsilon^{1/2}\left\{\frac{4+15\tilde{f}_1^{\mathrm{crit}}}{12} + \frac{9\tilde{f}_1^{\mathrm{crit}}}{4}\frac{(\tilde{f}_d^{\mathrm{crit}} - \tilde{f}_{d+1}^{\mathrm{crit}})(9\tilde{f}_1^{\mathrm{crit}} - \tilde{f}_d^{\mathrm{crit}})}{(3\tilde{f}_1^{\mathrm{crit}} - \tilde{f}_d^{\mathrm{crit}})^2}\right\} \end{aligned} \tag{5.35}$$

and the similar expansion

$$\begin{aligned} \tilde{W}'_d &= \left\{\frac{2-3\tilde{f}_1^{\mathrm{crit}}}{9\tilde{f}_1^{\mathrm{crit}}} + \log\left(\frac{3}{2}\frac{(3\tilde{f}_1^{\mathrm{crit}} - \tilde{f}_{d+1}^{\mathrm{crit}})}{(3\tilde{f}_1^{\mathrm{crit}} - \tilde{f}_d^{\mathrm{crit}})}\right)\right\} \\ &\quad - \tilde{C}(Z)\sqrt{\tilde{\nu}}\,\epsilon^{1/2}\left\{\frac{2+3\tilde{f}_1^{\mathrm{crit}}}{6} + 9(\tilde{f}_1^{\mathrm{crit}})^2\frac{(\tilde{f}_d^{\mathrm{crit}} - \tilde{f}_{d+1}^{\mathrm{crit}})}{(3\tilde{f}_1^{\mathrm{crit}} - \tilde{f}_d^{\mathrm{crit}})(3\tilde{f}_1^{\mathrm{crit}} - \tilde{f}_{d+1}^{\mathrm{crit}})}\right\}. \end{aligned} \tag{5.36}$$

In the fixed n ensemble, we deduce that the ratio $\tilde{W}'_d|_{g^n}/\tilde{W}'_\infty|_{g^n}$ tends at large n to the cumulative distribution function for d:

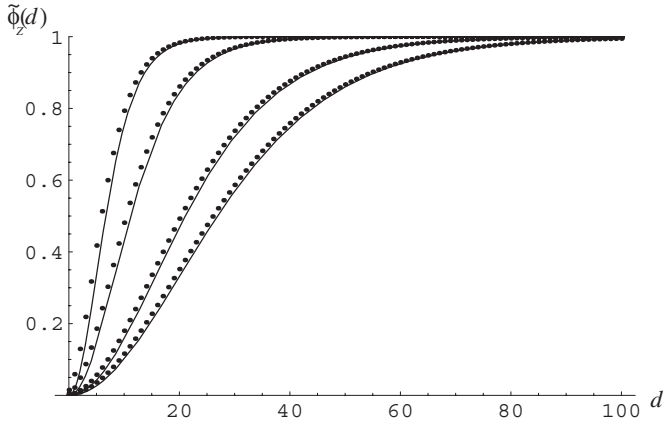

Figure 14. Plots of the (non-universal) cumulative distribution function $\tilde{\phi}_Z(d)$ for Z approaching the critical value $2/9$ from above, namely $Z = 0.23$, 0.225, 0.223 and 0.2227 (dotted plots from left to right). Beside each plot, we display the corresponding (universal) limiting scaling form (solid line) of equation (5.38).

$$\begin{aligned}\tilde{\phi}_Z(d) &= 1 + \frac{54\big(\tilde{f}_1^{\rm crit}\big)^2}{2+3\tilde{f}_1^{\rm crit}} \frac{\big(\tilde{f}_d^{\rm crit} - \tilde{f}_{d+1}^{\rm crit}\big)}{\big(3\tilde{f}_1^{\rm crit} - \tilde{f}_d^{\rm crit}\big)\big(3\tilde{f}_1^{\rm crit} - \tilde{f}_{d+1}^{\rm crit}\big)} \\ &= 1 - \frac{27x(1+x+x^2)}{(2+x)^2(1+2x)^2}\left\{1 - \frac{\big(\frac{2+x}{1+2x} - x^d\big)\big(\frac{2+x}{1+2x} - x^{d+1}\big)}{\big(\frac{2+x}{1+2x} + x^d\big)\big(\frac{2+x}{1+2x} + x^{d+1}\big)}\right\} \\ &\quad \text{with } x = \tilde{x}_{\rm crit}(Z). \end{aligned} \tag{5.37}$$

Note that this distribution is different from the distribution $\phi_z(d)$ of equation (4.39) obtained for a non-self-avoiding boundary. When Z approaches the critical value $2/9$, however, we have

$$\tilde{\phi}_Z(d) \sim \tanh^2(d\,\tilde{\beta}(Z)) \quad \text{with} \quad \tilde{\beta}(Z) = \tfrac{3}{2}\sqrt{Z - \tfrac{2}{9}}, \tag{5.38}$$

and we recover the universal scaling form of equation (4.40). The function $\tilde{\phi}_Z(d)$ is plotted against its scaling form (5.38) for $Z = 0.23$, 0.225, 0.223 and 0.2227 in figure 14.

Finally, to study the regime $Z \sim 2/9$, we can set

$$\begin{aligned} g &= \tfrac{1}{12}(1 - \mu\,\epsilon) \\ Z &= \tfrac{2}{9}(1 - \tilde{\mu}_B\,\epsilon^{1/2}) \\ d &= D\,\epsilon^{-1/4} \end{aligned} \tag{5.39}$$

if we work with a fixed value of Z, or alternatively replace the second equation by

$$p = P\,\epsilon^{-1/2} \tag{5.40}$$

if we work in a fixed p ensemble. In the first ensemble, we have the expansion

$$\begin{aligned} \tilde{W}_d - (\tilde{W}_0 - 1) &= \tfrac{3}{2}\left(1 - \epsilon^{1/4}\mathcal{H}\,(D;\mu,\tilde{\mu}_B/3) + \cdots\right) \\ \tilde{W}'_d - (\tilde{W}_0 - 1) &= \log\left(\tfrac{3}{2}\right) - \epsilon^{1/4}\mathcal{H}\,(D;\mu,\tilde{\mu}_B/3) + \cdots \end{aligned} \tag{5.41}$$

with $\mathcal{H}$ as in (4.52), while $\tilde{W}_0 = 4/3 + \mathcal{O}(\epsilon^{1/2})$. We thus recover the *same scaling function* as that obtained for non-self-avoiding boundaries, with a simple renormalization of the 'boundary cosmological constant' by $1/3$.

In the fixed length ensemble, we obtain from (5.19) the scaling behavior

$$\frac{\tilde{W}_d|_{Z^p}}{(9/2)^p} \sim \epsilon^{3/4}\frac{9}{4}\bar{\mathcal{H}}(D;3P;\mu) \tag{5.42}$$

with $\bar{\mathcal{H}}$ as in (4.59). Except for the trivial factor $9/4$, we recover again the same scaling function as that obtained for non-self-avoiding boundaries, with now a renormalization of the perimeter by a factor of 3. As for $\tilde{W}'_d$, since it has the same singular behavior as $\tilde{W}_d$ up to a factor $3/2$, we deduce

$$\frac{\tilde{W}'_d|_{Z^p}}{(9/2)^p} \sim \epsilon^{3/4}\frac{3}{2}\bar{\mathcal{H}}(D;3P;\mu). \tag{5.43}$$

This behavior can also be obtained directly by taking the scaling limit of (5.20).

After going to the fixed n ensemble and taking the appropriate ratio $\tilde{W}'_d|_{g^n Z^p}/\tilde{W}'_\infty|_{g^n Z^p}$, we now find that

$$\bar{\Phi}_{\substack{\text{self-avoiding}\\ \text{boundary}}}(D,P) = \bar{\Phi}(D,3P) \tag{5.44}$$

for the distribution function for D in the fixed p ensemble.

Note that the ratio $\tilde{W}_d|_{Z^p}/\tilde{W}'_d|_{Z^p}$ tends to $3/2$ which may be interpreted as the asymptotic average number of boundary vertices closest to the origin in the case of a self-avoiding boundary. This number is independent of D in the scaling regime.

To conclude, large quadrangulations with a self-avoiding boundary behave essentially as large quadrangulations with a non-self-avoiding boundary, as far as the bulk–boundary distance is concerned. For boundary lengths of the order $n^{1/2}$, quadrangulations with a self-avoiding boundary of length P behave as quadrangulations with a non-self-avoiding boundary of length $3P$. This suggests that, in quadrangulations with a non-self-avoiding boundary, only one of the irreducible components is macroscopic and has a boundary of length equal to $1/3$ of the total perimeter, while all the other components are microscopic but altogether, the lengths of their boundaries represent $2/3$ of the total perimeter.

6. Self-avoiding loops

We end this paper by a study of the statistics of distances in *quadrangulations with a self-avoiding loop*. As already discussed in section 2, a self-avoiding loop is a closed path made of consecutive edges of the quadrangulation, which is simple, i.e. visits any vertex at most once. For convenience, we shall suppose that the loop is oriented. Upon cutting along the loop, we obtain two quadrangulations with a self-avoiding boundary, constrained to have the same perimeter. The orientation allows us to distinguish these two pieces as left and right. We can now express a number of generating functions for this problem in terms of the generating functions found in section 4.

A first simple generating function is that of quadrangulations with a self-avoiding loop with a marked vertex on the loop. It reads immediately

$$\Omega_0(g,y) = \sum_{p\geqslant 1} y^p (\tilde{W}_0(g,Z)|_{Z^p})^2, \tag{6.1}$$

where g is the weight per face while $\sqrt{y}$ is a weight per edge of the loop (the length of the loop is necessarily even).

Another interesting quantity involving the distance is the generating function for quadrangulations with a self-avoiding loop with a marked vertex at distance *less than or equal to d*, lying to the right of the loop (or possibly on the loop itself). It reads

$$\Omega_d(g,y) = \sum_{p\geqslant 1} y^p \tilde{W}_0(g,Z)|_{Z^p}\tilde{W}'_d(g,Z)|_{Z^p} \tag{6.2}$$

if the configurations are counted with their usual inverse symmetry factor. This can be seen by first noting that the generating function for the same objects with an additional marking of a closest vertex on the loop is obviously given by $\sum_{p\geqslant 1} y^p \tilde{W}_0(g,Z)|_{Z^p} \tilde{W}_d(g,Z)|_{Z^p}$ upon gluing the two boundaries in such a way that their marked vertices coincide. Removing the marked closest vertex, we see that a given configuration is over-counted by a factor of k equal to the number of closest vertices on the loop. Dividing by this factor k amounts to replacing $\tilde{W}_d$ by $\tilde{W}'_d$ as in section 4. Note that, clearly, the quantity Ω_d is related to the quantity Γ_d of section 2 by

$$\Gamma_d = \Omega_d - \Omega_{d-1}, \qquad \Gamma_0 = \Omega_0. \tag{6.3}$$

From the exponential growth $\tilde{W}_0 \sim (9/2)^p$ and $\tilde{W}'_d \sim (9/2)^p$, we immediately deduce that a transition occurs now at $y = y_{\rm crit}$ with

$$y_{\rm crit} = \left(\tfrac{2}{9}\right)^2 = \tfrac{4}{81}. \tag{6.4}$$

For $y < 4/81$, the typical values of p contributing to $\Omega_d(g,y)$ remain finite when g tends to its critical value $1/12$. Setting

$$\begin{aligned} g &= \tfrac{1}{12}(1-\mu\,\epsilon) \\ d &= D\,\epsilon^{-1/4}, \end{aligned} \tag{6.5}$$

we may use (5.27) and (5.28) to write

$$\begin{aligned} \Omega_d|_{y^p} = 4\left(\frac{4}{9}\right)^p \left(\frac{(3p-3)!}{p!(2p-1)!}\right)^2 + 2\left(\frac{4}{9}\right)^p \frac{(3p-1)!}{p!(2p)!}\,\frac{(3p-3)!}{p!(2p-1)!} \\ \times\left\{1-3p\,\mathcal{F}(D;\mu)\,\epsilon^{1/2}+\cdots\right\} \end{aligned} \tag{6.6}$$

for $p \geqslant 1$. Summing over p with a weight y^p, we obtain

$$\begin{aligned} \Omega_d &= a(y) - b(y)\mathcal{F}(D;\mu)\,\epsilon^{1/2}+\cdots \\ &\text{with}\quad a(y) = 2\sum_{p\geqslant 1}\left(\frac{4}{9}\right)^p y^p \frac{(3p-3)!}{p!(2p-1)!}\left(2\frac{(3p-3)!}{p!(2p-1)!}+\frac{(3p-1)!}{p!(2p)!}\right) \\ &\qquad b(y) = 6\sum_{p\geqslant 1}\left(\frac{4}{9}\right)^p y^p \frac{(3p-3)!}{(p-1)!(2p-1)!}\,\frac{(3p-1)!}{p!(2p)!}, \end{aligned} \tag{6.7}$$

which are functions of y with no singularity for $y < 4/81$. Going to a fixed n ensemble and considering large values of n, we immediately deduce from the singular behavior (6.7) that the cumulative distribution function for the rescaled distance $D = d/n^{1/4}$ from the marked vertex in the bulk to the self-avoiding loop is again, in the regime $y < y_{\rm crit}$, equal to the universal two-point function $\Phi(D)$ of the Brownian map, as given by equation (4.22). In this regime, the size of the loop does not scale with n and becomes negligible in the large n limit.

In the regime $y > 4/81$, we expect that the dominant singularity corresponds to large values of p. In this case, we may use (5.16) and (5.20) to write the large p behavior

$$\begin{aligned} \Omega_d|_{y^p} &\sim \left(\frac{27gR^3}{4}\right)^{2p} \frac{1}{\pi\,(3p)^3}\left(\frac{1}{3f_1}-1\right)\left\{\left(\frac{1}{3f_1}-1\right)+\frac{3}{2}\left\{1-2\sum_{k=1}^{\infty}\frac{(f_{d+1})^k-(f_d)^k}{(3f_1)^k}\right\}\right\} \\ &= \left(\frac{27gR^3}{4}\right)^{2p} \frac{1}{\pi\,(3p)^3}\left(\frac{(1-3f_1)(2+3f_1)}{18f_1^2}\right)\left\{1+\frac{54f_1^2}{2+3f_1}\,\frac{f_d-f_{d+1}}{(3f_1-f_d)(3f_1-f_{d+1})}\right\}. \end{aligned} \tag{6.8}$$

The line $y(27gR^3/4)^2 = 1$ defines the critical value $\hat{g}_{\rm crit}(y)$ of g for $y > y_{\rm crit}$, namely

$$\hat{g}_{\rm crit}(y) = \tilde{g}_{\rm crit}(\sqrt{y}) \tag{6.9}$$

with $\tilde{g}_{\rm crit}(Z)$ as in equation (5.22). Upon summing over p with a weight y^p, the p-dependent prefactor gives rise when $((27/4)g\,R^3)^2\,y \to 1$ to a singularity

$$-\frac{1}{2}\left(1-\left(\frac{27g\,R^3}{4}\right)^2 y\right)^2 \log\left(1-\left(\frac{27g\,R^3}{4}\right)^2 y\right) \propto \left(1-\frac{g}{\hat{g}_{\rm crit}(y)}\right)^2 \log\left(1-\frac{g}{\hat{g}_{\rm crit}(y)}\right). \tag{6.10}$$

This singularity translates into an asymptotic behavior of the form $(\hat{g}_{\rm crit}(y))^{-n}\,/n^3$ for $\Omega_d|_{g^n}$ at large n, with a multiplicative factor proportional to the d-dependent coefficient in (6.8), taken at $x = x(\hat{g}_{\rm crit}(y)) = \tilde{x}(\sqrt{y})$. Note that this d-dependent coefficient comes from $\tilde{W}_d'$ only and we therefore recover in the fixed n ensemble (and in the regime $y > 4/81$) the same form (5.37) for the cumulative distribution function $\tilde{\phi}_Z(d)$ for d provided we identify $Z = \sqrt{y}$ in this formula.

The most interesting situation is when y is in the vicinity of $4/81$. Alternatively, we may work in the fixed length ensemble and study the scaling limit (6.5) with moreover

$$p = P\,\epsilon^{-1/2}. \tag{6.11}$$

In this limit, we may use the relation (5.43) and the relation

$$\frac{\tilde{W}_0|_{Z^p}}{(9/2)^p} \sim \epsilon^{5/4}\,2\frac{{\rm e}^{-3\sqrt{\mu}P}}{\sqrt{\pi}(3P)^{5/2}}(1+3P\sqrt{\mu}) \tag{6.12}$$

inherited from (5.16) to deduce that

$$\begin{aligned}\frac{\Omega_d|_{Z^p}}{(81/4)^p} &\sim \epsilon^2\,3\frac{{\rm e}^{-3\sqrt{\mu}P}}{\sqrt{\pi}(3P)^{5/2}}(1+3P\sqrt{\mu})\bar{\mathcal{H}}(D;3P;\mu)\\ &= \epsilon^2\hat{\mathcal{H}}(D,P;\mu) \quad \text{with}\\ \hat{\mathcal{H}}(D,P;\mu) &= 3\frac{{\rm e}^{-6\sqrt{\mu}P}}{\pi(3P)^4}(1+3P\sqrt{\mu})\left\{1+\left(3\sqrt{\mu}-2f^2(D;\mu)\right)\int_0^\infty {\rm d}K\,{\rm e}^{-\frac{K^2}{3P}-2f(D;\mu)K}2K\right\},\end{aligned} \tag{6.13}$$

involving a *new universal scaling function* $\hat{\mathcal{H}}(D,P;\mu)$.

For small P, we have

$$\hat{\mathcal{H}}(D,P;\mu) \overset{P\to 0}{\sim} \tfrac{3}{\pi(3P)^4}(1-(3P)\mathcal{F}(D;\mu)+\cdots) \tag{6.14}$$

which matches the large p behavior of $\Omega_d|_{y^p}$ in the regime $y < 4/81$. For large P, we have instead

$$\hat{\mathcal{H}}(D,P;\mu) \overset{P\to\infty}{\sim} 3\frac{{\rm e}^{-6\sqrt{\mu}\,P}}{\pi(3P)^3}\sqrt{\mu}\tanh^2\left(\sqrt{\frac{3}{2}}\,\mu^{1/4}\,D\right). \tag{6.15}$$

If we now turn to the fixed n ensemble, in the limit of large n, with the scaling

$$p = P\,n^{1/2}, \tag{6.16}$$

we get a cumulative distribution function

$$\hat{\Phi}(D,P) = \frac{18P^3\sqrt{\pi}}{1+18P^2}\,{\rm e}^{9P^2}\int_{-\infty}^{\infty}{\rm d}\xi\,\frac{\xi}{\rm i}\,{\rm e}^{-\xi^2}\,\hat{\mathcal{H}}(D,P;-\xi^2), \tag{6.17}$$

which measures the probability that a vertex chosen uniformly at random in the quadrangulation with a self-avoiding loop of rescaled length $2P$ be at a rescaled distance less than D from this loop. This is a new universal distribution which cannot be reduced to the distribution $\bar{\Phi}(D,P)$

of previous sections by a simple rescaling of P. It is plotted in figure 4 for $P = 0.01, 0.1, 0.2, 0.5$ and 1.0. For small D and fixed P, we have the expansion

$$\hat{\Phi}(D, P) = \frac{9}{2} P\, D^2 - \frac{3}{2} \frac{1 + 9P^2 + 162P^4}{1 + 18P^2} D^4 + \cdots. \tag{6.18}$$

From (6.14), we see that $\hat{\Phi}(D, P) \to \Phi(D)$ at small P for fixed D, as expected. From (6.15), and via a saddle point estimate of the integral over ξ, we find that, for $P \to \infty$, the typical value of D is of order $P^{-1/2}$, with the scaling form

$$\hat{\Phi}(D, P) \sim \tanh^2\left(\sqrt{\tfrac{9}{2}} D \sqrt{P}\right), \tag{6.19}$$

i.e. we recover the general form found in previous sections.

7. Discussion and conclusion

To briefly summarize our results, we have been able to find discrete exact expressions for the bulk–boundary and boundary–boundary correlators for quadrangulations with a generic boundary. In the case of a self-avoiding boundary, we have been only able to express the bulk–boundary correlator, leading eventually to results for a model of self-avoiding loop. From our discrete expressions, we identified three scaling regimes for which we gave the asymptotic behaviors.

Most of the above results follow from the discovery of the 'master formula' (2.5) for W_d, which is remarkable in itself. This is yet another manifestation of the still mysterious integrability of the equations governing distance statistics in maps, as already observed for the two-point and three-point functions. Here two levels of integrability are involved, first for the equation determining R_d, involving the parameter g only, and then for equation (3.6) determining W_d, involving z and R_d as an 'external potential'. In this respect, it is worth mentioning that we have a continued fraction expansion

$$W_d = \cfrac{1}{1 - \cfrac{z R_{d+1}}{1 - \cfrac{z R_{d+2}}{\cdots}}} \tag{7.1}$$

and furthermore, we have the conserved quantity

$$W_d - g\, z\, R_d R_{d+1} R_{d+2} W_d W_{d+1} W_{d+2} = W - g\, z\, R^3 W^3 \qquad \text{for all} \quad d. \tag{7.2}$$

This identity may be checked directly from the explicit expression (3.12) for W_d. Alternatively, using (3.5) to expand both sides of this equation in powers of z, it is equivalent to an infinite number of conserved quantities involving R_d and g only, and it is easy to check that those correspond precisely to the conserved quantities found in [28].

Another remarkable fact is the strong similarity, already apparent at the discrete level, between the bulk–boundary correlators for generic and self-avoiding boundaries. Unfortunately, we have not been able to exhibit the same phenomenon for boundary–boundary correlators. Furthermore, had we gone over this problem, we are still far from understanding the distance statistics between two points lying on a self-avoiding loop: the loop and geodesics may cross each other, which prevents the decoupling of both sides observed in (6.2) for the bulk–loop correlator.

Our universal expressions are properties of what could be called the Brownian map with a boundary. In this respect, we may wonder whether these results may be re-obtained in a purely continuous formalism, which would likely require a proper probabilistic definition

of this object. At a more physical level, we note that the expression (4.78) may be re-derived from the solution $\mathcal{P}(D, U; \mu)$ of some diffusion equation in a potential $\mathcal{F}(D; \mu)$ as in equation (4.11):

$$\frac{\partial}{\partial U}\mathcal{P} = \frac{\partial^2}{\partial D^2}\mathcal{P} - \mathcal{F}\mathcal{P}. \tag{7.3}$$

Here $\mathcal{P}$ describes the law of the position D at time U of a particle diffusing in the potential $\mathcal{F}$ in one spatial dimension. Discarding normalization factors, it reads

$$\mathcal{P}(D, U; \mu) \propto \frac{\mathrm{e}^{-\sqrt{\mu}U}}{U^{5/2}}\,\mathrm{e}^{-\frac{D^2}{4U}}(D^2 - 2U + 2UDf(D; \mu)), \tag{7.4}$$

with $f(D; \mu)$ as in (4.7). The expression (4.78) can be obtained by considering the quantity $\mathcal{P}(D, U; \mu)\mathcal{P}(D, P - U; \mu)$, setting $\mu = -\xi^2$ and performing the usual appropriate integral over ξ to go to a fixed area ensemble, and finally introducing the rescaled variables $\delta = D/\sqrt{P}$ and $u = U/P$. Heuristically, $\mathcal{P}(D, U; \mu)\mathcal{P}(D, P - U; \mu)$ is the continuous counterpart of the generating function for Dyck paths of fixed length, constrained to reach some prescribed height at some given step. The potential $\mathcal{F}(D; \mu)$ is the continuous counterpart of the weight R_d attached to each descent $d \to d - 1$ of the Dyck path.

To conclude, let us list a few possible generalizations of our results. We expect integrability to survive when considering maps with faces of degrees other than 4, as found for the two-point function in [12]. We may also consider maps of higher genus and/or with several boundaries. For instance, [6] and [7] give continuous results for surfaces with two boundaries at a prescribed mutual distance, for which discrete formulae may as well exist. Finally, introducing multiple boundaries may pave the way for understanding the distance statistics in the general $\mathbf{O}(\mathcal{N})$ loop model on dynamical random lattices.

References

[1] Kazakov V 1985 Bilocal regularization of models of random surfaces *Phys. Lett.* B **150** 282–4
David F 1985 Planar diagrams, two-dimensional lattice gravity and surface models *Nucl. Phys.* B **257** 45–58
Ambjørn J, Durhuus B and Fröhlich J 1985 Diseases of triangulated random surface models and possible cures *Nucl. Phys.* B **257** 433–49
Kazakov V, Kostov I and Migdal A 1985 Critical properties of randomly triangulated planar random surfaces *Phys. Lett.* B **157** 295–300

[2] Tutte W 1962 A census of planar triangulations *Can. J. Math.* **14** 21–38
Tutte W 1962 A census of Hamiltonian polygons *Can. J. Math.* **14** 402–17
Tutte W 1962 A census of slicings *Can. J. Math.* **14** 708–22
Tutte W 1963 A census of planar maps *Can. J. Math.* **15** 249–71

[3] Brézin E, Itzykson C, Parisi G and Zuber J-B 1978 planar diagrams *Commun. Math. Phys.* **59** 35–51

[4] For a review, see: Di Francesco P, Ginsparg P and Zinn–Justin J 1995 2D gravity and random matrices *Phys. Rep.* **254** 1–131

[5] Polyakov A M 1981 Quantum geometry of bosonic strings *Phys. Lett.* B **103** 207–10
Polyakov A M 1981 Quantum geometry of fermionic strings *Phys. Lett.* B **103** 211–3

[6] Ambjørn J and Watabiki Y 1995 Scaling in quantum gravity *Nucl. Phys.* B **445** 129–44 (arXiv:hep-th/9501049)

[7] Ambjørn J, Jurkiewicz J and Watabiki Y 1995 On the fractal structure of two-dimensional quantum gravity *Nucl. Phys.* B **454** 313–42 (arXiv:hep-lat/9507014)

[8] Ambjørn J, Durhuus B and Jonsson T 1997 *Quantum Geometry: A Statistical Field Theory Approach* (Cambridge: Cambridge University Press)

[9] Marcus M and Schaeffer G 2001 Une bijection simple pour les cartes orientables, available at http://www.lix.polytechnique.fr/Labo/Gilles.Schaeffer/Biblio/; see also
Schaeffer G 1998 Conjugaison d'arbres et cartes combinatoires aléatoires *PhD Thesis* Université Bordeaux I
Chapuy G, Marcus M and Schaeffer G 2007 A bijection for rooted maps on orientable surfaces arXiv:0712.3649 [math.CO]

[10] Bouttier J, Di Francesco P and Guitter E 2004 Planar maps as labeled mobiles *Electron. J. Comb.* **11** R69 (arXiv:math.CO/0405099)
[11] Bouttier J, Di Francesco P and Guitter E 2007 Blocked edges on Eulerian maps and mobiles: application to spanning trees, hard particles and the Ising model *J. Phys. A: Math. Theor.* **40** 7411–40 (arXiv:math.CO/0702097)
[12] Bouttier J, Di Francesco P and Guitter E 2003 Geodesic distance in planar graphs *Nucl. Phys.* B **663** 535–67 (arXiv:cond-mat/0303272)
[13] Chassaing P and Schaeffer G 2004 Random planar lattices and integrated super-Brownian excursion *Probab. Theory Relat. Fields* **128** 161–212 (arXiv:math.CO/0205226)
[14] Miermont G and Weill M 2008 Radius and profile of random planar maps with faces of arbitrary degrees *Electron. J. Probab.* **13** 79–106 (arXiv:0706.3334 [math.PR])
[15] Marckert J F and Mokkadem A 2006 Limit of normalized quadrangulations: the Brownian map *Ann. Probab.* **34** 2144–202 (arXiv:math.PR/0403398)
[16] Le Gall J F 2007 The topological structure of scaling limits of large planar maps *Invent. Math.* **169** 621–70 (arXiv:math.PR/0607567)
[17] Le Gall J F and Paulin F 2008 Scaling limits of bipartite planar maps are homeomorphic to the 2-sphere *Geom. Funct. Anal.* **18** 893–918 (arXiv:math.PR/0612315)
[18] Miermont G 2008 On the sphericity of scaling limits of random planar quadrangulations *Electron. Commun. Probab.* **13** 248–57 (arXiv:0712.3687 [math.PR])
[19] Bouttier J and Guitter E 2008 Statistics of geodesics in large quadrangulations *J. Phys. A: Math. Theor.* **41** 145001 (arXiv:0712.2160 [math-ph])
[20] Miermont G 2009 Tessellations of random maps of arbitrary genus *Ann. Sci. Éc. Norm. Supér.* (at press) (arXiv:0712.3688 [math.PR])
[21] Le Gall J-F 2008 Geodesics in large planar maps and in the Brownian map *Acta Math.* (at press) (arXiv:0804.3012 [math.PR])
[22] Bouttier J and Guitter E 2008 The three-point function of planar quadrangulations *J. Stat. Mech.* P07020 (arXiv:0805.2355 [math-ph])
[23] Bouttier J and Guitter E 2009 Confluence of geodesic paths and separating loops in large planar quadrangulations *J. Stat. Mech.* P03001 (arXiv:0811.0509 [math-ph])
[24] Di Francesco P 2004 Applications of random matrices to physics *2D Quantum Gravity, Matrix Models and Graph Combinatorics* (*Lecture Notes given at the Summer School*) (France: Les Houches) (arXiv:math-ph/0406013)
[25] Aldous D 1993 Tree-based models for random distribution of mass *J. Stat. Phys.* **73** 625–41
[26] Kostov I 1988 O(n) vector model on a planar random lattice: spectrum of anomalous dimensions *Mod. Phys. Lett.* A **4** 217–26
[27] Goulden I P and Jackson D M 1983 *Combinatorial Enumeration* (New York: Wiley)
[28] Di Francesco P and Guitter E 2005 Integrability of graph combinatorics via random walks and heaps of dimers *J. Stat. Mech.* P09001 (arXiv:math/0506542 [math.CO])